Inelastic sputtering of solids by ions

1988 Sov. Phys. Usp. 31 1015

(http://iopscience.iop.org/0038-5670/31/11/R03)

Inelastic sputtering of solids by ions

I. A. Baranov, Yu. V. Martynenko, S. O. Tsepelevich, and Yu. N. Yavlinskiĭ

I. V. Kurchatov Institute of Atomic Energy, Moscow
V. G. Khlopin Radium Institute, Academy of Sciences of the USSR, Leningrad
Usp. Fiz. Nauk **156**, 477–511 (November 1988)

A review is given of both theoretical and experimental investigations of the sputtering as a result of strong excitation of the electron subsystem of a solid by fast and multiply charged ions. A systematic account is given of the main experimentally established relationships governing inelastic sputtering. An analysis is made of the dependences of the inelastic sputtering coefficient on the energy and charge of the incident ions and on the target structure, and of the differential characteristics of the sputtered particles. Theoretical investigations of the electron-excitation region and its relaxation, of the transfer of the electron energy to the target atoms, and of the inelastic sputtering models are discussed. A brief account is given of the history of the topic, of possible practical applications of inelastic sputtering, and of its relationship to other phenomena.

CONTENTS

1. INTRODUCTION

Interaction of fast ($\sim 10^9$ cm/s) and multiply charged ions with condensed matter can erode the surface because of the excitation of the electron subsystem (this is known as inelastic sputtering).

A material can be sputtered if an atom or a group of atoms acquires an energy sufficient to detach itself from the surface. In traditional sputtering this energy is transferred by a bombarding particle as a result of elastic collisions and the cascade of subsequent elastic collisions of the displaced atoms increases the number of those atoms that acquire an energy sufficient for detachment from the surface.[1] However, if the electron subsystem of a solid is excited, then at first sight it would seem that its atoms would not receive sufficient energy. This follows from the fact that the electron relaxation times are short and the transfer of the electron energy to atoms is a slow process because of the ratio of the electron and atomic masses. Therefore, for a long time it has been assumed that inelastic processes have no role in sputtering.

The first direct proof of inelastic sputtering was provided by experiments reported in Refs. 2 and 3, where it was shown that in the range of energies where the nuclear stopping power $(dE/dx)_n$ decreases on increase in the energy and the electron stopping power $(dE/dx)_e$ rises, the sputtering coefficients of americium oxide and plutonium hydroxide increase with the fission fragment energy. This was in conflict with the well-tested cascade theory of sputtering and all the data on this fairly thoroughly investigated phenomenon[4] and it demonstrated that there is also sputtering as a result of inelastic energy losses. Further investigations involving bombardment of metals, metal oxides and fluorides, solidified gases, and organic materials by fission fragments and fast ions have demonstrated that inelastic sputtering is indeed possible and it differs from traditional sputtering in respect of the relationships governing it and physical mechanisms. The inelastic sputtering coefficients (representing the number of atoms removed from the surface by one ion) can be orders of magnitude greater than the values typical of the elastic sputtering process. For example, in the first report of inelastic sputtering[4] the coefficient S representing the sputtering of uranium and plutonium by fission fragments was one or two orders of magnitude higher than the expected values.

In accounting for the process of inelastic sputtering we must first of all answer the question as to how the excitation energy of electrons is transferred to atoms in a solid and what is the relaxatiom time of such electron excitation.

It is now clear that electron excitations in metals relax due to electron heat conduction and that the characteristic relaxation time is much shorter than the time for the transfer

 0038-5670/88/111015-20$01.80

of the electron energy to the lattice. In insulators there are no free electrons outside the excited region and, because of the Coulomb attraction and necessary quasineutrality, electrons cannot leave the excited region. The motion of an excitation boundary is due to ionization of atoms by electron impact and is in the form of an ionization wave moving at a velocity $U \propto d_0/\tau$, where d_0 is the Debye radius of electrons inside the excited region and τ is the ionization time. Such relaxation is much slower than in metals and it occurs in a time comparable with the time for the transfer of the electron energy to the lattice.

There are various views on the transfer of energy to the atoms in the lattice, which is the process that determines the inelastic sputtering mechanism: these views can be divided arbitrarily into two groups. In the thermal spike model the stress is on the likely mechanisms of heating of the lattice to temperatures needed to detach atoms from the surface. On the other hand, the Coulomb explosion model deals with the possibility of acceleration of ions in an electric field.

It is very likely that the thermal spike model is directly applicable only to insulators, whereas in metals the process of lattice heating is possible only in fine-grained targets when the grain size is $\lesssim 10$ nm. Fast ions can then detach whole grains. The idea of a Coulomb explosion, i.e., of expulsion of ions from a region which loses some electrons as a result of excitation, is not self-consistent in its direct form, since in metals the charge is rapidly compensated by conduction electrons and in insulators the charge is distributed on the boundary of the excitation region. However, a double electrical layer exists on the surface of a metal and in this layer the pressure $E^2/8\pi$ exerted by an electric field is balanced by the pressure of excited electrons $P \approx nT_e$. The field intensity $E = T_e/d_0$ can then be sufficient to ensure that during the lifetime of hot electrons the ions acquire an energy sufficient for detachment from the surface.

The difference between the inelastic and elastic sputtering mechanisms naturally results in a difference between the physical relationships governing these effects. The energy dependence of the inelastic sputtering coefficient $S(E)$ reduces basically the dependence of the inelastic losses $(dE/dx)_e$ and the coefficient obeys $S \propto (dE/dx)_e^{\alpha}$, where $\alpha = 2$–4. In some cases the relationship between S and $(dE/dx)_e$ is not single-valued and inelastic sputtering depends also on the energy spectrum of excited electrons.

Inelastic sputtering of insulators is usually much stronger than that of metals. Elastic sputtering depends weakly on the electron structure of the target.

It is characteristic that inelastic sputtering of fine-grained materials with a grain size of $\lesssim 10$ nm is 2–3 orders of magnitude stronger than in the case of coarse-grained targets.

When large grains are sputtered inelastically, a considerably higher proportion of the sputtered particles and also of the particles sputtered in the form of large clusters or molecules is charged. The particles sputtered as a result of inelastic excitation emerge mainly at right-angles to the surface.

Studies of inelastic sputtering have shown that the mechanisms explaining this effect are not exotic, but are manifested in many effects in solid-state physics.

Excitation of electrons in a solid resulting in inelastic sputtering is observed in two cases: 1) irradiation of a solid with fast ions which are retarded by interaction with electrons in the medium and the nuclear stopping power is small; 2) irradiation with slow multiply charged ions which are characterized by a high potential energy of neutralization.

The potential energy of a multiply charged ion is equal to the sum of the ionization potentials of the missing electrons and for ions of $q \sim 20$ charge it amounts to 20–30 keV. The outer electron shells are filled in a solid or near its surface as a result of the Auger processes and the energy released excites electrons.

Excitation of the electron subsystem in a solid also occurs as a result of high-intensity irradiation with laser or electron beams, but in this case the energy density is less than in the case of inelastic sputtering by multiply charged ions. In spite of some general similarity of the processes occurring in these two cases, there are some essential differences and the available models cannot be applied directly from one case to the other.

The processes of neutralization of slow multiply charged ions and retardation of fast ions in a solid are similar. The only difference is that a slow multiply charged ion creates a spherical excited region near the surface, whereas a fast ion for which the electron energy losses are greater than the nuclear ones creates a cylindrical excitation region. Moreover, a characteristic time for the excitation of electrons by a fast ion is $\sim 10^{-16}$ s, whereas the Auger neutralization time is $\sim 10^{-14}$ s and is comparable with the cooling time of electrons due to heat conduction. Inelastic sputtering by slow multiply charged ions has not been investigated much[5-6] and the charge of the ions used in such sputtering has not exceeded $q = 9$. Experimental facilities for the investigations of sputtering by ions with higher values of q had only just become available.[7]

Sputtering of some nonconducting materials is possible also when electron and photon beams are used. However, in this case the excitation or ionization applies to single electrons and is not a collective process. Sputtering by electrons and photons, frequently called electron sputtering, is discussed in Ref. 8. Therefore, in the present review the attention is concentrated on the excitation of an electron subsystem when the collective processes predominate. The term *inelastic sputtering* should be used in this specific case.

2. PASSAGE OF FAST IONS THROUGH MATTER

Inelastic sputtering has been investigated experimentally for solids irradiated with fast ions when the inelastic energy losses $(dE/dx)_e$ exceeds greatly the elastic losses $(dE/dx)_n$. Figure 1 shows schematically the dependence of the energy losses experienced by an ion on its energy E. In

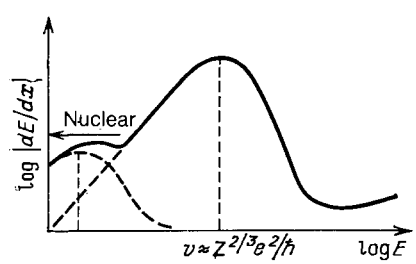

FIG. 1. Schematic dependence[4] of dE/dx on the ion energy E.

the range of low energies the predominant processes are the elastic losses due to the scattering of ions by atoms in a solid, whereas at high energies we have $(dE/dx)_e > (dx/dx)_n$.

If the velocity of an ion is less than the Bohr velocity $v < e^2/\hbar$, this ion travels inside a solid in the form of an atom and inelastic losses are governed by the exchange of electrons between a moving atom and electrons in the solid. The characteristic energy for the excitation of electrons in the case of such deceleration is $mv^2/2$, where m is the electron mass. If the velocity of an ion is higher than the velocity of the outer electrons, then a moving ion carries an equilibrium charge q_{eq} equal to the number of electrons whose orbital velocity is less than v. In the Thomas-Fermi model we have

$$q_{eq} = Z_i^{1/3} \frac{\hbar v}{e^2}, \quad (1)$$

where Z_i is the atomic number of the ion. However, the establishment of an equilibrium charge of an ion incident on a target characterized by $q \neq q_{eq}$ requires a certain finite time and electrons are captured by an ion with $q > q_{eq}$ more slowly than they are detached if $q < q_{eq}$.

An ion with a charge q is slowed down because of the polarization of the medium, leading to excitation of plasmons[9] of energy $\hbar\omega_p$ $[\omega_p = (m/4\pi ne^2)^{-1/2}]$.

If the velocity of an ion exceeds the velocity of electrons in an atom, the atoms in a medium may become ionized. The ionization losses increase on increase in the ion velocity since such an increase makes it possible to excite a larger number of electrons. However, if the velocity of an ion exceeds the electron velocity corresponding to a certain average ionization potential ($v \approx Z_a^{2/3} e^2/\hbar$, where Z_a is the atomic number of atoms in the target), the inelastic losses decrease on increase in the ion velocity and this is due to the Coulomb scattering cross section at high velocities. In this case we have the familiar Bethe-Bloch expression

$$-\left(\frac{dE}{dx}\right)_e = \left(\frac{4\pi q^2 e^4}{mv^2}\right) Z_a N \ln \frac{2mv^2}{J}. \quad (2)$$

In the range of velocities where the ionization energy losses predominate it is found that both $(dE/dx)_e$ and the spectrum of excited electrons are independent of electrical properties of the target (metal or insulator). The stopping power $(dE/dx)_e$ depends strongly on the ion charge. For example, in the case of a proton in typical solid targets the value of $(dE/dx)_e$ does not exceed ~ 100 eV/nm, whereas in the case of a fission fragment of velocity $\sim 10^9$ cm/s with a mass ~ 100 a.m.u. and a charge $q \sim 20$, we have $(dE/dx)_e \approx 10^4$ eV/nm.

The screening of the ion charge at velocities $v \geqslant e^2/\hbar$ occurs at distances $\sim v/\omega$, where $\omega = \omega_p$ for metals, whereas $\omega = g/\hbar$ for insulators; g is the width of the band gap. Since v/ω exceeds the impact parameters for which electrons can acquire a significant energy, the interaction of an ion with electrons can be regarded as of the Coulomb type. Therefore, the spectrum of primary excited electrons dn_e/dE decreases at high energies in the same way as the spectrum of free electrons, $dn_e/dE \propto E^{-2}$, whereas at low values of E we find that dn_e/dE has a maximum at an energy of the order of several ionization potentials J. The complete spectrum of excited electrons is found by summing over all the electrons excited from different electron shells. It is important to note that the maximum energy which an excited electron can have is $E_{max} \approx (4m/M)E$, where M is the mass of an ion, which is very different in the case of light and heavy ions: for a fission fragment we have $E_{max} \approx 2$ keV, whereas for protons of energy 10 MeV, the corresponding energy is $E_{max} \approx 40$ keV.

Atoms with vacancies in their inner shells are formed due to the passage of a fast ion and these shells are filled as a result of the Auger processes in a time $\sim 10^{-14}$ s. However, since the cascade Auger processes are the most probable (they involve consecutive transitions to the nearest lower level), the excited Auger electrons have relatively low energies.

Inelastic sputtering and the formation of tracks as well as radiation-induced chemical reactions are governed not only by the inelastic losses $(dE/dx)_e$, but also by the excited-electron spectrum.

The simplest and most characteristic parameter is the average energy density Q released in the electron subsystem. When calculated per one atom, this energy density is

$$Q = \left(\frac{dE}{dx}\right)_e (\pi R^2 N)^{-1}, \quad (3)$$

here R is the characteristic size of a cylindrical region (we usually have $R \ll L$, where L is the range of an ion) where the excitation is localized.

An excited primary electron of energy E moves the following distance from the ion track[10]:

$$r(E) = \lambda(E) \sin\theta = \lambda(E) \left(1 - \frac{E}{E_{max}}\right)^{1/2}, \quad (4)$$

where θ is the angle between the ion track and the electron momentum. The dependence of the range λ of an electron on its energy is a practically universal function which applies to various materials (Fig. 2). A typical value of R is obtained by averaging $r(E)$ for a given spectrum of excited electrons. Since $R(E)$ increases on increase in E, particularly in the case of light ions, the maximum of $Q(E)$ is shifted toward lower energies compared with the maximum of $(dE/dx)_e$.

In the case of plasmon excitation,[12] we have

$$R = \max\left[\frac{\pi v}{\omega_p}, \lambda_p\right], \quad (5)$$

where $\pi v/\omega_p$ is the impact parameter corresponding to the appearance of a plasmon and λ_p is its range, i.e., the distance in which a plasmon decays into one-particle excitations.

The energy density Q depends strongly on the param-

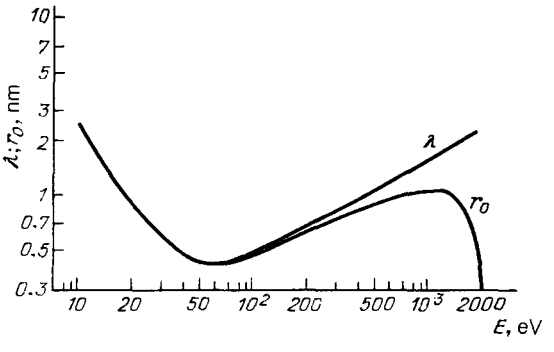

FIG. 2. Mean free path λ of primary electrons[11] and their distance r_0 from a fission fragment track[10] plotted as a function of the electron energy.

eters of an ion. In the case of fission fragments the density Q exceeds 100 eV/atom, which is considerably greater than the Fermi energy ε_F, the width of the band gap g in insulators, and the ionization potentials of the outer electron shells. In the case of light ions (such as protons) we have $Q \leqslant 10^{-2}$–10^{-3} eV/atom.

3. EXPERIMENTAL INVESTIGATIONS OF INELASTIC SPUTTERING

The demonstration of the existence of inelastic sputtering in the early seventies was followed by a wide range of experiments which made it possible to establish the main relationships governing this phenomenon and to demonstrate its difference from sputtering as a result of elastic collisions. For example, the energy dependence of the inelastic sputtering coefficient $S(E)$ mainly follows the energy dependence of inelastic losses represented by $(dE/dx)_e$. However, the correspondence between $S(E)$ and $(dE/dx)_e$ is not single-valued because inelastic sputtering is also governed by the spectrum of the energies of excited electrons.

In contrast to elastic sputtering, which is practically independent of the charge state of the bombarding ions, the sputtering due to inelastic energy losses depends on the charge of an ion incident on a target. However, this is manifested only if the depth at which an equilibrium charge of an ion traveling inside a target is established exceeds the thickness of the layer responsible for the sputtering.

A characteristic feature of inelastic sputtering is in some cases a strong dependence on the target structure. The inelastic sputtering coefficient of some fine-grained samples with a grain size of ~ 10 nm is several orders of magnitude greater than that of coarse-grained targets. Since this may imply the existence of special sputtering mechanisms, the structure of the investigated target material should be taken into account in discussing the relationships governing inelastic sputtering.

The electron structure of a target subjected to inelastic sputtering is manifested much more strongly than in the elastic case so that we have to consider separately the relationships governing sputtering of metals and insulators.

Moreover, the differential characteristics of inelastic sputtering are distinct: this applies to the distribution of the sputtered particles in respect of their masses, energies, and angles of emergence from the target. In the case of inelastic sputtering the fraction of charged sputtered particles is considerably greater and the mass distribution includes clusters containing hundreds and thousands of atoms.

3.1. Dependence of the inelastic sputtering coefficient on the ion energy

The dependence of the inelastic sputtering coefficient on the ion energy $S(E)$ was first determined in Ref. 2. Experiments were carried out on a fine-grained film of AmO_2 prepared by evaporation in vacuum on a metal substrate. The sputtered material was deposited on a collector and the amount of it was deduced from the α-activity of americium. The bombarding particles were fragments resulting from the fission of ^{252}Cf nuclei: the energies of the light fragments were ~ 100 MeV and those of heavy fragments were ~ 80 MeV. The fragment energy was altered by their deceleration in metal films of different thicknesses (Fig. 3d). Throughout the full range of energies, both in the case of heavy and light fragments, the value of $(dE/dx)_e$ increased on increase in the ion energy, whereas $(dE/dx)_n$ decreased. The dependence of the sputtering coefficient on the average fragment energy $\langle E \rangle$ plotted in Fig. 3a demonstrated an increase in S on increase in $\langle E \rangle$ and therefore was evidence of inelastic sputtering. A similar result under better experimental conditions and with a film thinner than that of ^{252}Cf was obtained for a fine-grained plutonium hydroxide $PuO_x(OH)_{4-2x}$ film formed by electrolysis on a metal substrate (Fig. 3b).[3] In the case of both americium dioxide and plutonium hydroxide the sputtering by fission fragments was characterized by $S = 3 \times 10^2$–3×10^3 atoms/ion, whereas the values of S calculated from the cascade theory were 3–4 atoms/ion. Therefore, the work reported in Refs. 2 and 3 was the first proof of the existence of sputtering as a result of inelastic processes. It should be stressed that the values of S obtained

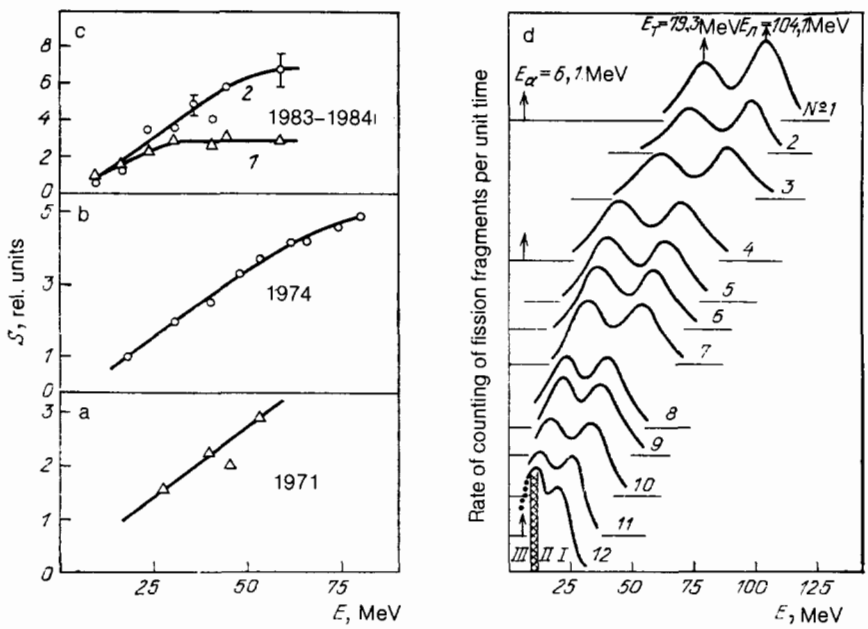

FIG. 3. Dependences of the sputtering coefficient S on the average kinetic energy of fission fragments $\langle E \rangle$ bombarding fine-grained films: a) AmO_2 (Ref. 2); b) $PuO_x(OH)_{4-2x}$ (Ref. 3); c) Au (Refs. 13 and 14); 1) gold film with an average grain size ~ 7 nm; 2) gold film with an average grain size ~ 14 nm. d) Energy spectra (Nos. 1–12) of fission fragments after passage through decelerating films. Spectrum No. 12: I), II) undistorted regions; III) part of the spectrum distorted by α particles from ^{252}Cf.

in Refs. 2 and 3 were total and represented the whole sputtered material and not some particular charged component.

Subsequently, the range of materials which could be sputtered by inelastic processes began to widen greatly. The energy dependence of the sputtering coefficient was used to draw conclusions on inelastic sputtering of the following materials: metals (Au) with a fine-grained structure (Fig. 3c),[13,14] metal oxides (UO_2, AmO_2) with a fine-grained structure,[2,15] metal fluorides (UF_4, AmF_3, CaF_3),[15] alkali halides (CsI, CsBr, KCl, etc.),[18–22] biomolecular compounds[18–22] in the form of ergosterol ($C_{28}H_{44}O$), glycylglycine ($C_4H_8O_3N_2$), valine ($C_5H_{12}O_2N$), phenylalanine ($C_0H_{11}O_2N$), and others, and also ice and solidified gases (H_2O, CO, CO_2, SO_2, CH_4, N_2, O_2, Ar, Xe, etc.).[17,23–28] A common feature of the energy dependences of the coefficients $S(E)$ of all these materials is that they repeat the overall nature of the dependence

$$\left[\frac{dE}{dx}(E)\right]_e.$$

Like the dependence

$$\left[\frac{dE}{dx}(E)\right]_e,$$

the dependence $S(E)$ for inelastic sputtering is dome-shaped (Fig. 4),[17] but a comparison shows that $S(E)$ rises more steeply than does $(dE/dx)_e$ on increase in E to the left of the maximum $(dE/dx)_e$ and falls even more steeply on increase in E to the right of the maximum of $(dE/dx)_e$. Figure 5, based on Ref. 18, shows the dependences of the yield of Cs obtained by sputtering CsI with various ions, on $(dE/dx)_e$. For each ion (^{16}O, ^{32}S, ^{63}Cu, ^{127}I) it was found that in a certain range of values of $(dE/dx)_e$ the coefficient obeyed $S \propto (dE/dx)_e^n$, where $2 \leqslant n \leqslant 4$. The different slopes of the dependences

$$S(E) \text{ and } \left[\frac{dE}{dx}(E)\right]_e$$

result in a double-valued dependence $S[(dE/dx)_e]$: the same values of $(dE/dx)_e$ but on opposite sides of the maximum of $(dE/dx)_e$ correspond to different values of S. At higher ion energies the value of S is considerably less to the right of the maximum of $(dE/dx)_e$. This "loop" effect is manifested clearly for the ^{16}O ions in Fig. 5 and is observed also for ^{32}S ions. It is also manifested by heavier ions, such as ^{63}MCu or ^{127}I but they must have much higher energies beyond the maximum of $(dE/dx)_e$.

The ion energy governs the spectrum of primary excited electrons, the radius of the excitation region R, and consequently the electron energy density. This is manifested by the fact that the maximum of the dependence of S on the ion energy E (Fig. 4) is shifted toward lower energies compared with curves representing the dependences

$$\left[\frac{dE}{dx}(v)\right]_e \quad \text{or} \quad \left[\frac{dE}{dx}(E)\right]_e.$$

This shift is greater for light ions which manifest more strongly the dependence of the energy density of excited

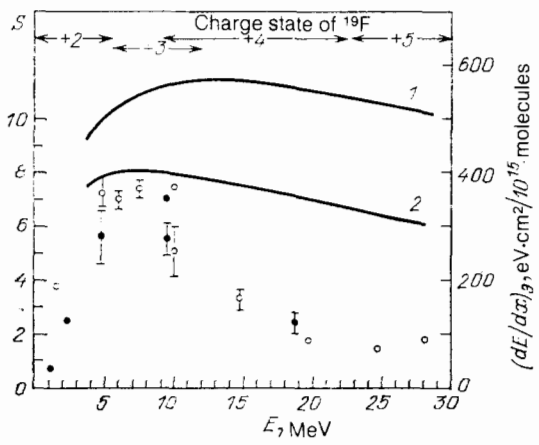

FIG. 4. Sputtering coefficients S of UF_4 (black dots) and of H_2O in the form of ice (open circles), plotted as a function of the fluorine ion energy.[17] The values of S for ice are reduced by a factor of 200. Curves 1 and 2 represent the electron stopping powers of UF_4 (reduced by a factor of 4) and of H_2O, respectively.[104]

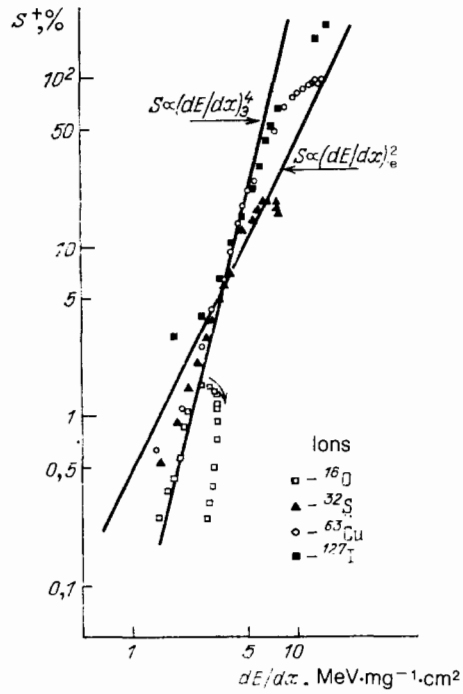

FIG. 5. Relative yields of CsI ions plotted as a function of the electron stopping power of CsI films sputtered by bombardment with ^{16}O, ^{32}S, ^{63}Cu, and ^{127}I ions.[18]

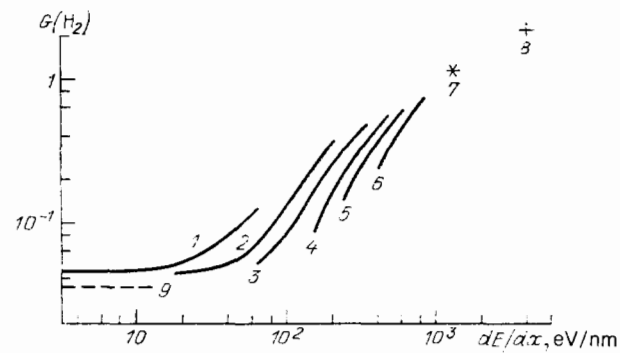

FIG. 6. Dependences of the differential radial yield of H_2 on $(dE/dx)_e$ obtained on irradiation of benzene[105] by H ions (1), He ions (2), Li ions (3), Be ions (4), B ions (5), C ions (6), Ne ions (7), fission fragments (8), and fast electrons (9).

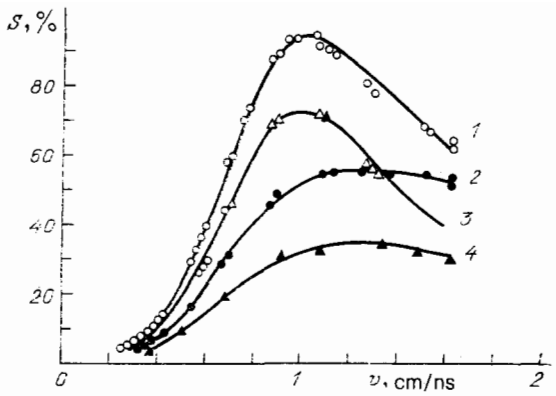

FIG. 7. Dependence of the yield of negative (1) and positive (2) ions of valine and of phenylalanine (curves 3 and 4) on the velocity v of the bombarding Cd ions.[22]

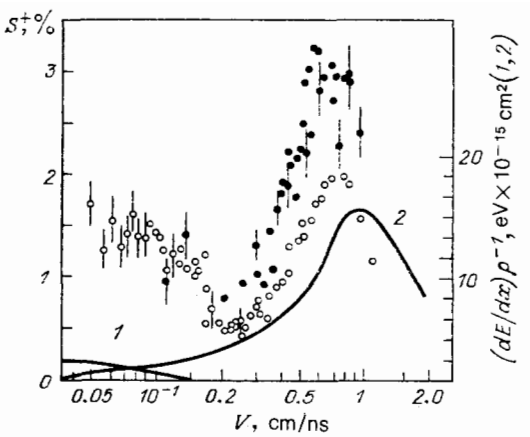

FIG. 8. Dependences of the yield of positive valine ions[21] of $(M + H)^+$ mass on the velocity v of oxygen and sulfur ions. Curves 1 and 2 represent the nuclear and electron stopping powers of valine for ^{16}O ions obtained from tables in Ref. 103 and expressions in Ref. 106.

electrons on R. It is interesting to note also the dependence[29] of the yield of hydrogen from benzene on $(dE/dx)_e$ for different ions (Fig. 6). This yield of H_2 depends strongly on the nature of the ion [for a given $(dE/dx)_e$] at low values of $(dE/dx)_e$ and for light ions, but the difference disappears in the case of heavy ions when the radius of the excited region depends weakly on the nature of the ion.

The dependence of the sputtering coefficient S on the density of the released energy Q is undoubtedly of interest. However, such dependences are usually not given because R is indeterminate. Moreover, one should note the discrepancy between the results given in various tables of $(dE/dx)_e$, which again complicates interpretation of the inelastic sputtering results.

We must bear in mind that when certain fine-grained materials are sputtered, we can expect saturation of the sputtering coefficient when $(dE/dx)_e$ exceeds the value at which an ion can sputter a grain. This was manifested, for example, in the sputtering of fine-grained (grain size ~ 7 nm) gold (curve 1 in Fig. 3c), whereas in the case of larger grains (~ 15 nm) the saturation has not yet been observed (curve 3 in Fig. 3c).

The dependences of the sputtering coefficients (ion component) of biomolecular compounds on the ion velocity are of the same nature (Fig. 7).[22] However, it is clear from Fig. 7 that in the case of positive and negative components the dependences of the yield of the sputtered particles on the ion velocity are different. Therefore, in the interpretation of the results we must bear in mind a possible difference between the behavior of the total sputtering coefficient and the coefficients representing the emission of charged particles. Interesting results are plotted in Fig. 8 (based on Ref. 21) which shows the transition from elastic sputtering of valine (at low velocities of ^{16}O and ^{32}S ions) to inelastic sputtering (at high velocities): a minimum of the dependence $S(v)$ is observed at $v = 2 \times 10^8$ cm/s.

The energy dependences of the sputtering coefficients of solidified gases are generally similar to the energy dependences of the inelastic sputtering coefficients of other materials. However, in the case of solidified gases sputtered by light ions it is found (Fig. 9)[27] that the dependence $S \propto (dE/dx)_e^{\alpha}$ is weaker and α lies within the range $1 \leqslant \alpha \leqslant 2$. It should be mentioned that, in spite of the approximately equal sublimation energies of solid Ar, N_2, and CO (0.083, 0.076, and 0.088 eV, respectively) the sputtering coefficients are very different (Figs. 9a, 9b, and 9c): $S \approx 10$ for N_2, $S \approx 50$ for Ar, and $S \approx 200$ for CO atoms or molecules per one He ion of energy 1.5 MeV. Sputtering of solid N_2 differs from the sputtering of solid rare gases and CO not only by the small value of S, but also by the fact that in the case of N_2 the dependence $S[(dE/dx)_e]$ shows the "loop" effect similar to that observed in the sputtering of CsI by ^{16}O ions (Figs. 9b and 5), whereas in the case of Ar and CO the dependences $S[(dE/dx)_e]$ show no such tendency (Figs. 9a and 9c). This is clearly due to the fact that the sputtering of solid rare gases and CO by light ions is dominated by the excitation of

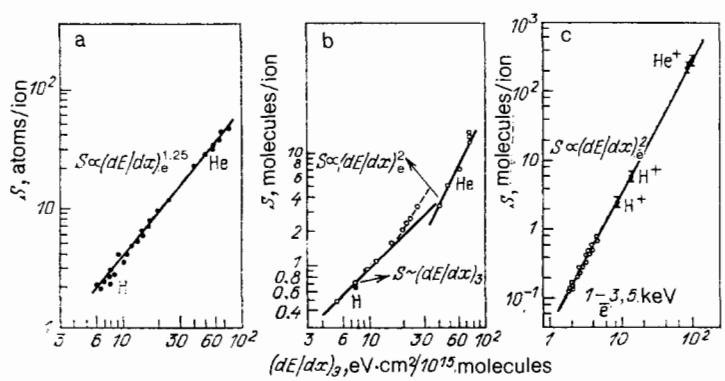

FIG. 9. Dependences $S[(dE/dx)_e]$ obtained for sputtering of Ar (a), N_2 (b), and CO (c) by hydrogen and helium ions and by electrons.[27]

individual electrons and not by collective processes. Therefore, the sputtering of Ar and CO is determined not by the density of the released energy, but by an integral of this energy in the surface layer of the target.

3.2. Dependence of inelastic sputtering on the charge of ions and their angle of incidence. "Backward" and "transmission" sputtering

A distinguishing feature of inelastic sputtering is its dependence on the initial charge of an ion q, governing the energy lost by fast ions $(dE/dx)_e$. The potential energy of a slow multiply charged ion also depends on q.

Sputtering of CsI, glycylglycine, and ergosterol by ^{16}O ions with different initial charges was reported in Ref. 19. The ion energy was 20 MeV in all cases, corresponding to the energies on the right of the maximum of

$$\left[\frac{dE}{dx}(E)\right]_e.$$

At this velocity the equilibrium charge is $q_{eq} \approx 6.5$. It is clear from Fig. 10 that in the range $q \leqslant 6$ the yield of the various ions depends weakly on their initial charge, whereas in the range $q > 6$ the experimental points fit well the dependence $S \propto q^4$. This result can be interpreted as follows. If the charge of the bombarding particle is less than the equilibrium value, its ionization to $q = q_{eq}$ is fast and it occurs at distances shorter than the depth of the layer responsible for the sputtering. Recombination of a fast ion with $q > q_{eq}$ is a slower process; characteristic distances can exceed the thickness of the layer governing sputtering. Therefore, if $q > q_{eq}$ the sputtering is due to ions with an initial charge close to q. Since in the investigated range of energies we have $(dE/dx)_e \propto q^2$, the observed dependence $S \propto q^4$ corresponds to $S \propto (dE/dx)_e^2$.

Similar results were obtained in studies of the sputtering of valine [30-32] and UF_4 (Ref. 17) by ^{16}O, ^{32}S, and ^{19}F ions. Although $S(q)$ was different from the results presented in Fig. 10, a general relationship was obeyed in all cases: if $q < q_{eq}$, it was found that S depended less strongly on q than

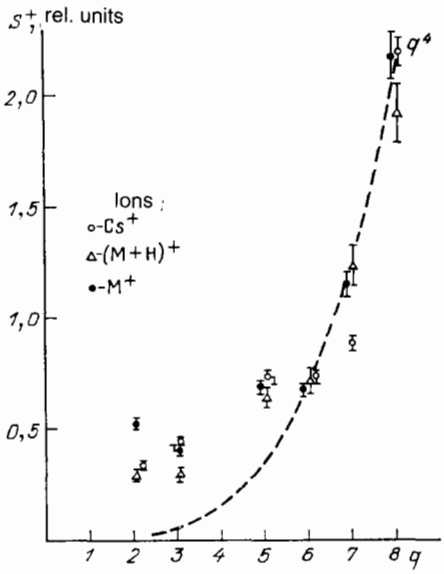

FIG. 10. Relative yields S^+ of positive Cs^+ ions from glycylglycine of mass $(M + H)^+$ and of ergosterol of mass M^+ plotted as a function of the individual charge q of the bombarding ^{16}O ions of energy 20 MeV, obtained by sputtering CsI, glycylglycine, and ergosterol.[19] The curves are normalized to the equilibrium charge of oxygen $q_{eq} = 6.5$.

for $q > q_{eq}$. It was pointed out in Ref. 17 that passage through a film resulted in some distribution of the ion charge because of the nonlinearity of $S(q)$ so that $\overline{S(q)} > S(\bar{q})$. Therefore, in the interpretation of the results and in determination of $(dE/dx)_e$ one should carefully measure the ion charge.

Inelastic sputtering of ZnS, LiF, NaCl, and Si crystals by slow multiply charged ions was also studied.[5,6] The ion emission coefficient was determined as a function of the ion energy and charge (Fig. 11). At low values $q = 1$–2 the kinetic ion emission was observed and its coefficient increased on increase in the ion energy. When the ion charge exceeded a certain threshold value ($q = 2$–3), the potential ion emission (i.e., inelastic sputtering) began. The potential ion

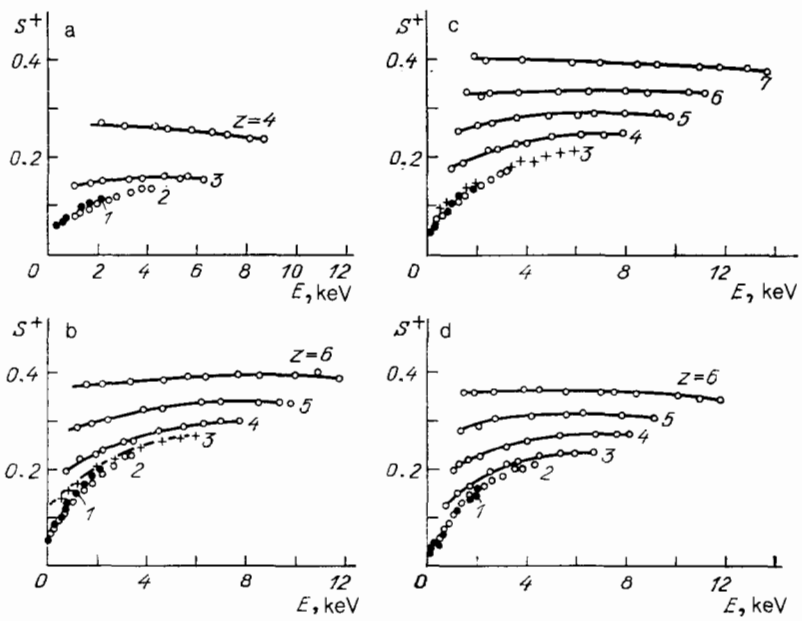

FIG. 11. Dependences of the coefficients S^+ of emission of Na^+ ions from an NaCl crystal on the energy of the bombarding Be^{z+} (a), Sb^{z+} (b), Cu^{z+} (c), and Re^{z+} (d) ions of different multiplicity z (Ref. 7).

emission coefficient S^+ increased on increase in q and there was a change in its dependence on the ion charge. At high values of q the coefficient S^+ was either independent of E or it fell on increase in E. When the ion velocity was increased, neutralization and excitation of electrons in the target occurred at a greater depth so that there was a reduction in the energy density transferred by electrons near the surface. Unfortunately, experiments on the sputtering by slow multiply charged ions have been relatively few and limited to low values of q.

There have been relatively few studies[15,19,33] of the dependence of inelastic sputtering on the angle of incidence θ of fast ions on a target. The $S(\theta)$ curves were approximated by $(\cos\theta)^{-n}$, where n was in the range $1 \leqslant n \leqslant 2$. Sputtering of fine-grained Au films by heavy multiply charged ions and fission fragments was characterized by $n = 1$. An increase in S with θ was attributed to sputtering of a large number of Au grains by one ion in the case when the incidence of ions on the surface became more of the grazing type.[15] A similar exponent $n = 1$ was obtained in a study[19] of the angular dependence of S^+ in the sputtering of positive Cs^+ ions from CsI and of glycylglycine bombarded with 20 MeV ^{16}O ions and 16 MeV ^{32}S ions. When the energy of ^{127}I ions was increased from 4 to 20 MeV, it was found[33] that the exponent in the angular dependence of S^+ for an ergosterol target changed from $n = 2$ to $n = 1$. The available experimental results are insufficient to establish a clear dependence of n on the nature of the target and on the parameters of an ion.

In some investigations[15,17,22,33,34] a comparison was made of inelastic sputtering in the "backward" direction relative to the ion beam and the sputtering of thin films by "transmission." In some experiments[15,17] the sputtering coefficients were found to be the same in both cases, but other authors[22,34] reported that the sputtering in the "transmission" case was stronger than in the "backward" direction. There was a tendency for the "transmission" sputtering to exceed the "backward" sputtering only at high energies. It would be premature to discuss the origin of these dependences.

3.3. Dependence of inelastic sputtering on the target structure

The inelastic sputtering coefficients of fine-grained targets (with the grain size in the range 5–10 nm) are considerably larger (by several orders of magnitude!) than the values of S for coarse-grained materials. This is the most characteristic feature of inelastic sputtering of a number of materials, such as metals, oxides, and some others.[35,36] One should point out that traditionally in studies of sputtering by fast ions $[(dE/dx)_e > (dE/dx)_n]$ or by nuclear fission fragment the targets had been fine-grained and formed by the deposition of thin films on substrates by evaporation in vacuum,[2,35–37] electrolysis,[2,3] or electrospraying.[18–22]

The use of fine-grained evaporated films and bulk targets in the study of sputtering has resulted in a large scatter of the sputtering coefficients.[35,36] It was shown in Ref. 37 that in the case of thin UO_2 films with the grain size ~ 7 nm the sputtering coefficient for fission fragments was $S \sim 10$ atoms/fragment, whereas in the case of bulk coarse-grained (~ 5 μm) targets,[38,39] it was found that $S = 5$–10 atoms/fragment.

The first direct investigations of the dependence of the inelastic sputtering process on the structure of a target were carried out on gold samples.[40] It was found that the sputtering coefficient of fine-grained gold films bombarded with ^{252}Cf fission fragments was $S \sim 10^3$ atoms/fragment, whereas for gold foil it was $S \sim 10$ atoms/fragment.

The most detailed investigations of the influence of the

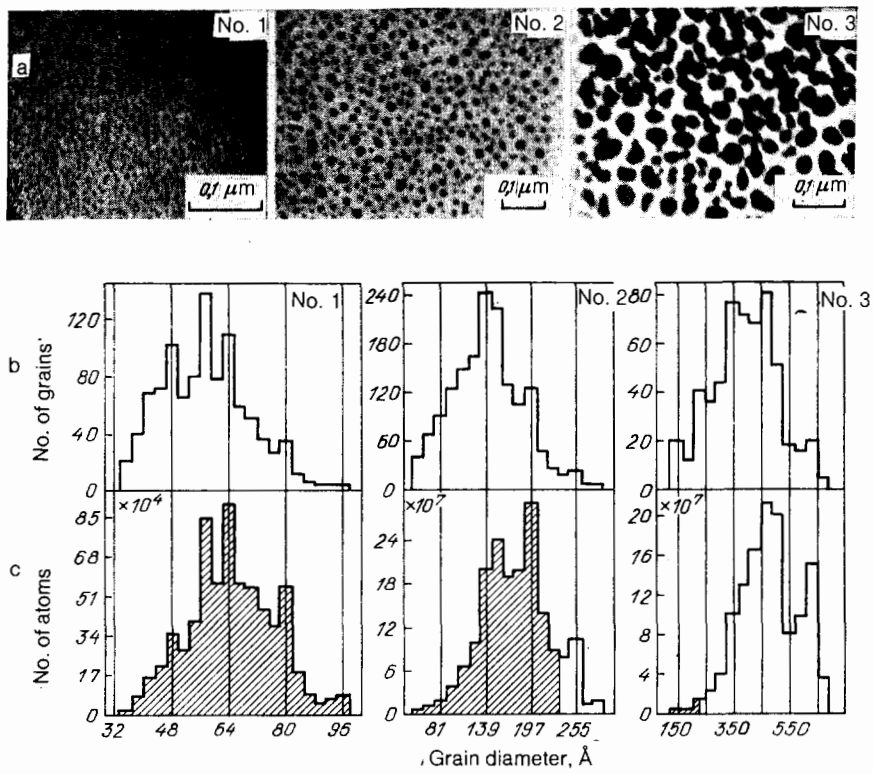

FIG. 12. Electron micrographs (a), distributions of the grain diameters of gold on a substrate (b), and distributions of atoms in grains of gold (c) obtained for three (Nos. 1–3) fine-grained gold targets.[41,42] The shaded regions represent those grain sizes which when included in the calculations ensure that the values of S agree with the experimental results for the sputtering by fission fragments.

TABLE I. Sputtering coefficients S of gold targets with different structures bombarded by fission fragments characterized by $(dE/dx)_e \approx 2000$–2300 eV/Å.

Target No.	1	2	3	4	5	6	7
Target surface structure	grain diameter 50–80 Å	grain diameter 100–200 Å	grain diameter 300–500 Å	flat islands ~1000 Å	annealed foil, 20 μm	annealed polycrystalline sample, 0.2 mm	bulk single crystal, (110) face
S, atoms/fragment	4000∓600	1100∓1800	42∓13	10∓4	15∓5	3∓1	7.0∓3.0
S_{calc}	2300	2100	2, 4	4	4	4	—
	S_e		S_n				

S_{calc} represents the electron coefficient S_e based on the model of an isolated grain[35,80] and S_n based on the model of Sigmund.[4]

target structure on inelastic sputtering were reported in Refs. 41 and 42. The sputtering was due to bombardment with ^{252}Cf fission fragments of gold targets with different grain size distributions (Fig. 12). The sputtering coefficients of these targets and also of a gold single crystal and heated coarse-grained polycrystalline gold samples are given in Table I, whereas the energy dependences $S(E)$ obtained for targets Nos. 1 and 2 are plotted in Fig. 3c. These experiments demonstrated that when a fission fragment hit a grain of size below a certain critical value, it was sputtered completely and the value of S increased with the grain size. The higher the fragment energy more accurately, the higher the value of $(dE/dx)_e$], the greater the critical grain size. For an average ^{252}Cf fission fragment the critical grain size was found to be ~25 nm. When the grain diameter exceeded ~25 nm, the sputtering coefficient was found to have the same value as for bulk coarse-grained gold and was comparable with the value predicted by the cascade theory in the case of elastic sputtering: 3–4 atoms/fission fragment.

However, the precision of the experimental and theoretical investigations is not yet sufficient to conclude that inelastic sputtering occurs in the case of coarse-grained metals. Most informative may be experimental studies of the energy dependences $S(E)$ in the range where $(dE/dx)_n$ decreases and $(dE/dx)_e$ rises on increase in the ion energy. On the other hand, $(dE/dx)_e$ should be sufficiently high because, as shown below, in the case of inelastic sputtering we must ensure that the density of the energy released to the electron subsystem exceeds a certain threshold value. Therefore, the experiments[20] in which the sputtering coefficients of Al and Cu were found to decrease on increase in the fragment energy were not informative because they were carried out using decelerated ^{252}Cf fragments [$v = (2$–$5) \times 10^8$ cm/s] and $(dE/dx)_e$ was less than the theoretically predicted threshold.

Inelastic sputtering of metal oxides UO_2, AmO_2, PuO_2, CfO_2, and AmF_3 was also found to depend on the target structure. Fine-grained samples were found to have a sputtering coefficient $S \sim 10^3$ atoms/fragment (Refs. 2, 3, 15, and 43–46), whereas coarse-grained samples had a coefficient $S \sim 10$ atoms/fragment (Refs. 35, 36, 38, and 39).

In the case of alkali halides, fluorides (UF_4, CaF_2), and organic compounds no special studies of the role of the target structure in inelastic sputtering had been made. A comparison of the various experiments[18,22] shows that the scatter of the values of S for targets of the same material did sometimes occur, but was considerably less than for metals and oxides.

It was thus found that the inelastic sputtering coefficients S were large for all materials in the fine-grained form. Coarse-grained metals and oxides had sputtering coefficients which did not differ from S obtained under elastic sputtering conditions.

In discussing the dependence of inelastic sputtering on the target structure it should be mentioned that in some cases[35–37,39,47–49] it was found that S decreased after a dose of $(2$–$3) \times 10^{12}$ cm^{-2} when fine-grained metal oxides were sputtered by fission fragments. This was due to preferential sputtering of fine grains and a reduction in their number and also due to grain enlargement as a result of their sintering during irradiation. On the other hand, when UF_4 films were sputtered by fluorine ions with an energy of 0.1–1.6 MeV/nucleon it was found that S was independent of the dose right up to that value when 30 atomic layers were sputtered.[16] This could indicate that inelastic sputtering of some materials (UF_4) was independent or weakly dependent on the target structure.

The dependences of S on the film thickness (d) for different materials reflected specific inelastic sputtering mechanisms. Since inelastic sputtering of metals and oxides was due to the size effect, S should depend on the degree of occupancy of the substrate area by grains (in the case of Au the grain size was ⩽20 nm). Therefore, the elementary "bricks" of a film were complete grains. Therefore, a rise of the dependence $S(d)$ in the case of fine-grained metals and oxides was very steep and when the average thickness of the film was 1–2 nm (3–4 μg/cm^2) in the case of Au or actinide oxides the values of S reached a plateau [44,45] before the substrate was completely covered.

The dependence $S(d)$ was different for inelastic sputtering of solidified rare gases (Ar,Xe).[24,25,27,28] In the case of Ar and Xe on a conducting substrate (Be) the value of S increased on increase in the thickness of the amorphous film up to $d \approx 100$ nm, whereas in the range $d \geqslant 100$ nm the coefficient S reached a certain constant value. On a nonconducting substrate (SF_6) the value of S decreased on increase in d, tending to the same constant value.

A similar slow rise of $S(d)$ was observed when Ar was sputtered[27] and this was true right up to $d = 100$ nm (sputtering of Ar and Xe was due to bombardment with H and He ions).

In the case of rare gases the dependence $S(d)$ was explained most plausibly[28] by diffusion of molecular Ar_2^+ ions and excited Ar_2^* molecules along the track of an ion. Nonradiative recombination of Ar_2^+ and deexcitation of Ar_2^* resulted in the transfer of energy to the atoms of Ar and, if this occurred on the surface, the atoms that received a sufficient kinetic energy became sputtered. On metal substrates both Ar_2^+ and Ar_2^* were lost because of recombination and deexcitation. A nonconducting substrate did not annihilate these molecules, but prevented their diffusion into the interior. Therefore, a metal substrate reduced the number of events of recombination of Ar_2^+ and deexcitation of Ar_2^*, resulting in sputtering, whereas a nonconducting substrate increased their number. The depth of the layer participating in the sputtering process was governed by the distances traveled by Ar_2^+ and Ar_2^* during their lifetime.

The same dependence of $S(d)$ as in the case of Xe and Ar was observed for KCl films sputtered by Ar ions of 70–300 keV energy and the thickness of the film at which S reached saturation was 200 nm (Refs. 50 and 51). On the other hand, in the case of solid N_2 and H_2O sputtered by H, He, C, and O ions of energy 1.5 MeV, there was no dependence $S(d)$ at least in the range $d \geqslant 10$–25 nm, indicating a different sputtering mechanism or a shorter diffusion excitation length.

Another target parameter important in the sputtering process is the temperature of the target. The dependence of inelastic sputtering on the target temperature has been investigated mainly for solidified gases[16,17,25,26,28,52] and also for KCl crystals.[53,54] In the case of SO_2, H_2O, CO_2, Ar, Xe, and so on it was found that below a certain temperature (characteristic of a given target material) the coefficient S was independent of T, whereas at higher temperatures an increase in T also increased S (Fig. 13).[26] In the case of CO_2 the temperature dependence $S(T)$ exhibited several upward steps and the height of these steps increased on increase in the CO_2 film thickness. Clearly, the target temperature in inelastic

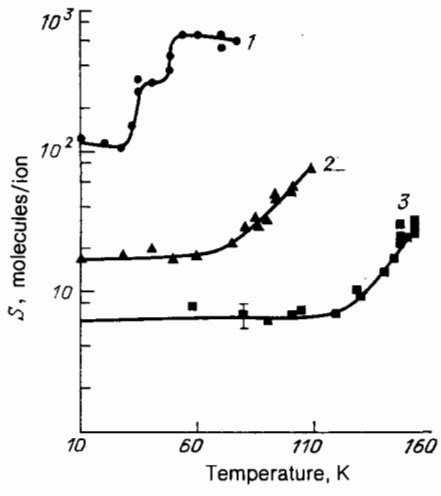

FIG. 13. Temperature dependences $S(T)$ obtained for the sputtering of CO_2 (1) SO_2 (2), and H_2O (3) films by 1.5-MeV He ions.

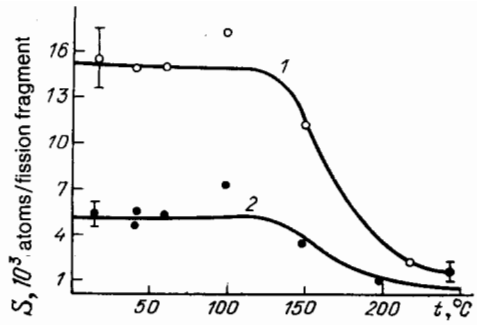

FIG. 14. Temperature dependences $S(T)$ for the sputtering of fine-grained Au films on metal substrates bombarded by ^{252}Cf fission fragments: 1) initial value $S = 1.5 \times 10^4$ atoms/ion; 2) initial value 5×10^3 atoms/ion.

sputtering of solidified gases and also of compounds such as KCl simply activated the diffusion of excited atoms or molecules.

Studies[16,17] of the sputtering of UF_4 by fluorine ions of energies 0.2–1.5 MeV/nucleon failed to reveal any dependence of the sputtering coefficient on the target temperature T right up to 200 °C.

In ultradisperse films of metals and oxides one would expect the small grains to coalesce at temperatures above 200 °C, which should affect the sputtering coefficient. For example, it was found that heating of ultradisperse Au films on metal substrates from 20 °C to 250 °C reduced S by a factor of 3–5 when T was increased from 150 °C to ~250 °C (Fig. 14). When measurements were repeated at 20 °C, the original value of S was not restored.

3.4. Distribution of the masses of sputtered particles

The distribution of the masses of sputtered particles is extremely important in determination of the sputtering mechanism and in practical applications of the process. The bulk of elastically sputtered particles leaves the target in the form of atoms. The proportion of sputtered molecules or atomic clusters is then low and it decreases rapidly on increase in the number of atoms in a cluster. However, inelastic sputtering is once again very different from the elastic process.

Initial studies of the sputtering of uranium oxide[37] and californium hydroxide[2] revealed that collectors of the sputtered material captured particles of size up to ~7 nm containing $\sim 10^4$ atoms. The sputtering was due to bombardment with fission fragments which emerged out of the target and the sputtered particles were studied using an electron microscope or solid-state track detectors. The presence of microscopic particles on collectors was mentioned also in later reports of other experiments.[35,36,55] However, these investigations could not be regarded as direct studies of the masses of the sputtered particles.

The mass spectrum of sputtered particles was determined for the first time with a time-of-flight mass spectrometer when biomolecular compounds were sputtered by ^{252}Cf fission fragments.[56,57] The mass spectra obtained in this case demonstrated that whole organic molecules were sputtered and these consisted of hundreds and thousands of atoms and their mass was 10^3–10^5 a.m.u. (Fig. 15). These investigations demonstrated the possibility of a new practical applica-

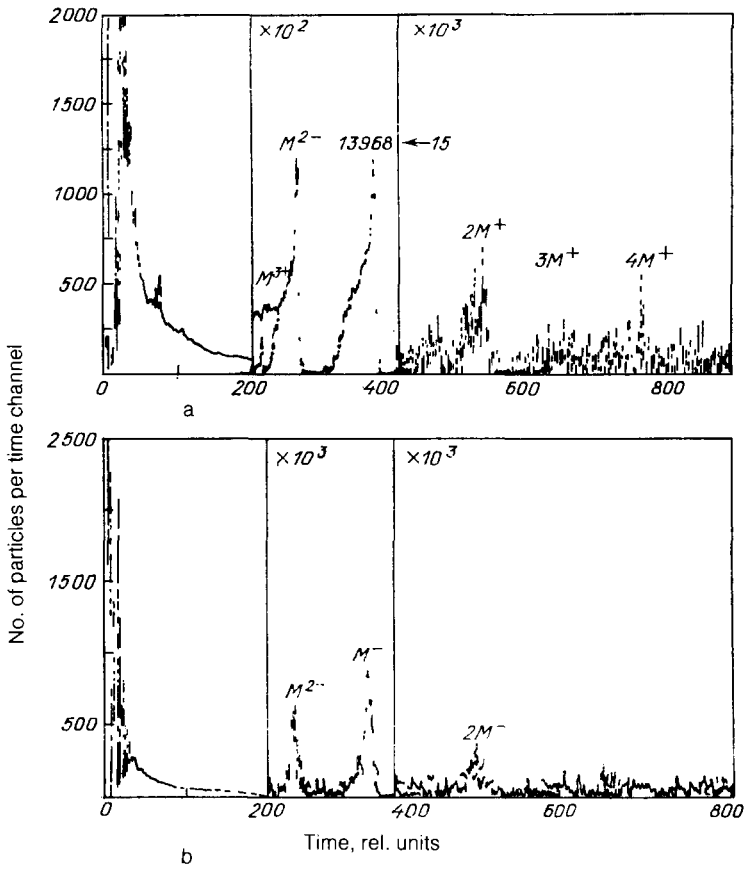

FIG. 15. Distribution of the masses of particles (the transit time given along the abscissa) obtained for positive (a) and negative (b) ions generated by sputtering a biomolecular compound film with a mass 13 968 a.m.u. (porcine phospholipase) by ^{252}Cf fission fragments.[58]

tion of inelastic sputtering which was generation of large ions of thermally unstable molecules of organic compounds. It is clear from Fig. 15 that the mass spectrum included molecular positive and negative ions with a charge up to 3, as well as particles of masses equal to two, three, and four molecules. A study of the dependence of the yield of ions of organic molecules of different masses and different size on the energy density delivered by an ion led to the conclusion[58,59] that the sputtering yield was affected more by the size of a molecule than by its mass.

An analysis of the mass spectrum obtained in the sputtering of UF_4 by ^{19}F ions of 5 MeV energy demonstrated[60] that the highest yield of ions was not in the form of atomic uranium or UF_4, but in the form of UF_2, $(UF_2)_2$, or $(UF_2)_3$.

Unfortunately, so far all the investigations of the mass distributions of the sputtered particles were confined to the charged components. Moreover, a direct comparison of the mass distributions of the particles sputtered from fine-grained and bulk samples has not yet been made, although theoretical models predict a considerable difference for these two cases. The sputtering products of fine-grained targets should be whole grains, whereas in the case of bulk samples they should be atoms.

In addition to the distribution of the masses of the sputtered particles, it is interesting to study their multiplicity, i.e., the number of particles sputtered by a single ion. The nunber of negative sputtered particles formed as a result of sputtering of CsI by uranium ions with an energy of 1.4 MeV/nucleon was determined.[22] The results are presented in Fig. 16, showing that each uranium ion sputtered on the average ~35 particles of different masses. The problems of multiplicity were discussed also in Refs. 18 and 62.

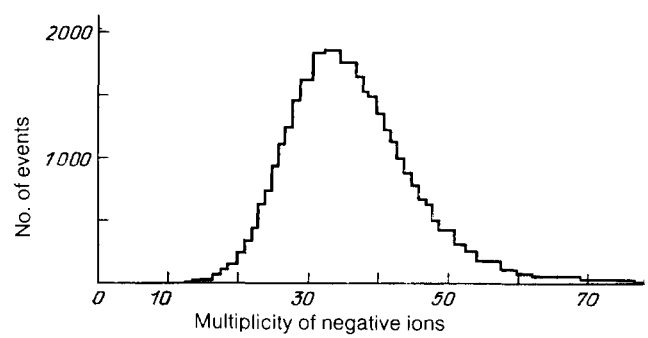

FIG. 16. Distributions of the multiplicity (number of negative ions of different mass sputtered simultaneously by an I^- ion) in bombardment of a CsI film by uranium ions of 1.4 MeV/nucleon energy.

3.5. Energy distributions of sputtered particles

In spite of the paucity of the experimental data on the energy distribution of particles, it had become clear that the average energy of the particles emerging from a target as a result of inelastic sputtering is low: 1–2 eV.

The energy distribution beyond the most probable energy exhibits a steeper fall than in the elastic sputtering case.

Figure 17 shows the energy spectra of the Cs^+ ions formed as a result of sputtering of CsI films by uranium ions of 1.4 MeV/nucleon energy.[61] The characteristic features of this spectrum are the most probable energy ~1.5 eV and the steep fall of the number of Cs^+ ions on increase in the energy. The same figure shows also the energy distribution of

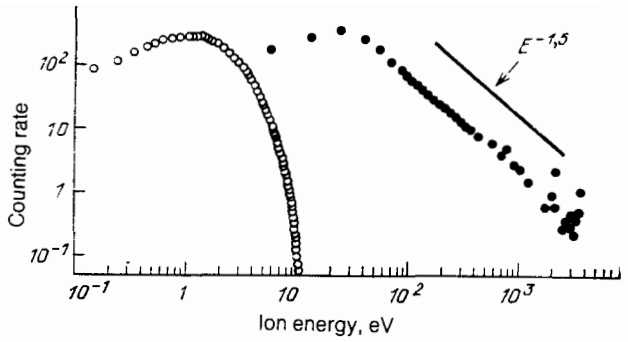

FIG 17. Energy distributions of Cs^+ ions (open circles) and of Al^+ ions (black dots) obtained by sputtering a thin CsI film and an aluminum foil substrate by bombardment with uranium ions of 1.5 MeV/nucleon energy (the calculated curve is based on the cascade model[4]).

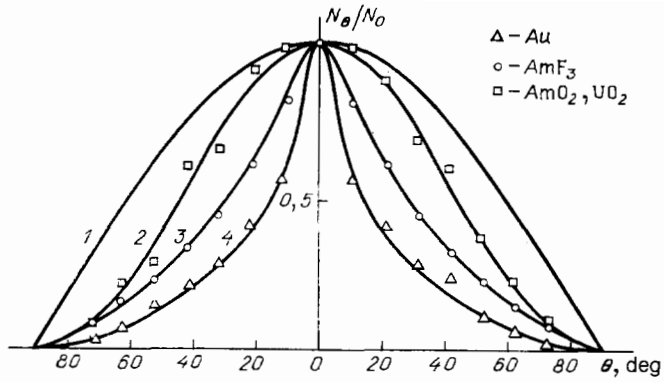

FIG. 18. Angular distributions of particles[15,63] sputtered by ^{252}Cf fission fragments from fine-grained films of Au [curve 4, $\exp(-2.2|\theta|)$], AmF_3 [curve 3, $\exp(-1.7|\theta|)$], AmO_2 and UO_2 [curve 2 represents $\cos^2\theta$ (Ref. 107) and curve 1 corresponds to $\cos\theta$].

ions obtained as a result of sputtering of an aluminum foil by uranium ions. This distribution is typical of the cascade mechanism in the case of elastic sputtering: the most probable energy of the positively charged component is tens of electron volts and the fall of the energy distribution on the high-energy side is proportional to $E^{-1.5}$. An energy spectrum similar to that shown in Fig. 17 was also reported for Cs^+ and Br^- ions generated as a result of sputtering of CsBr by ^{252}Cf fission fragments.[62]

The energy distribution of negatively charged particles (representing ~80% of all the emitted particles) obtained in a study of the sputtering of fine-grained gold by ^{252}Cf fission fragments was determined by the retarding potential method.[43,63] The energy spectrum was found to have a maximum at ~1.5 eV and at higher energies it differed from the E^{-2} spectrum, typical of elastic sputtering, and from the Maxwellian spectrum by a steeper fall.

The Maxwellian distribution of positive ions with temperatures of 3600 °C and 5200 °C was obtained when UF_4 was sputtered by fluorine ions of 5 and 13 MeV energies, respectively.[17] However, these temperatures were calculated on the assumption that only the U^+ ions were recorded. If the UF_2^+ or $(UF_2)_2^+$ and $(UF_2)_3^+$ ions had emerged preferentially, as mentioned before, then the temperature corresponding to the distribution would have to be higher than that given in Ref. 17.

Unfortunately, the precision and reliability of the available experimental data is insufficient to reveal any dependence of the energy spectra of the sputtered particles on the target composition and structure.

3.6. Angular distributions of sputtered particles

General size-effect features of the angular distributions of particles obtained as a result of inelastic sputtering are the preferential emission of particles along the normal to the target surface and independence of the angular distributions of the angle of incidence of ions on the target.[15,43,63] However, even in these cases the angular distributions may differ, depending on the target properties and structure. Figure 18 shows the angular distributions of particles sputtered from fine-grained films of gold, metal oxides (UO_2 and AmO_2), and americium fluoride. The narrowest distribution was obtained for particles of sputtered gold, it was wider for AmF_3 particles, and the widest for the sputtering of UO_2 and AmO_2. However, all these cases were characterized by the preferential emission of particles along the normal to the surface, in contrast to isotropic sputtering.

The observed angular distributions could clearly be explained by the combination of two sputtering mechanisms: detachment of grains from fine-grained targets should give rise to a narrow angular distribution, whereas evaporation (governing the sputtering of insulators) should be characterized by a $\cos\theta$ distribution. It should be mentioned that the angular distributions of particles obtained on sputtering of UF_4, when S was independent or weakly dependent on the film structure, by ^{19}F ions of ~5 MeV energy was described by the $\cos\theta$ law.[16]

3.7. Charge composition of sputtered particles

An investigation of the charge state of sputtered particles was made for Au (Refs. 63 and 64) and AmO_2, UO_2, or AmF_3 (Ref. 15). All the investigated targets were fine-grained films which were sputtered by ^{252}Cf fission fragments. In the elastic sputtering case the fraction of charged particles did not exceed 1% in most cases, whereas in the inelastic sputtering case the yields of charged and neutral particles were of the same order of magnitude. The proportion of negatively charged particles was particularly high in the case of sputtering of gold. The charge composition of the particles sputtered from gold was independent of the nature of the substrate (Ni, C, Au, Pt, NaCl) [63,64] This property was probably due to the fact that whole grains rather than single particles were sputtered. An important role should then be played by the properties of small particles and, in particular, by the dependence of the work function on the gold grain size.[65] The major proportion of charged particles obtained as a result of inelastic sputtering was evidence of the difference between this process and elastic sputtering. Bearing in mind also a high proportion of large particles in the sputtered material, we would expect inelastic sputtering to be useful in generation of ultraheavy (10^3–10^7 a.m.u.) ions.

The available experimental data thus demonstrate a significant difference between inelastic and elastic sputtering. However, there are differences between the relationships describing inelastic sputtering of different objects: metals, insulators, solidified gases; fine- and coarse-grained targets. Although a considerable amount of experimental data has already been accumulated, a complete picture cannot yet be provided of inelastic sputtering phenomena.

4. THEORETICAL INVESTIGATIONS OF INELASTIC SPUTTERING

In order to understand the nature of inelastic sputtering, we must answer the following questions: What is the nature of the region where electrons are excited? How does this region relax? How does an atom or a group of atoms acquire an energy sufficient for sputtering?

We shall now consider the formation of an excitation region in metals and insulators, then relaxation of this region, and the sputtering of metals and separately of insulators because of the difference between the physical processes occurring in them.

4.1. Excitation region

An important characteristic was introduced earlier Eq. (3)]: it is the energy density Q in the electron subsystem near the track of a fast ion. In some investigations[66,67] the known spectrum of electrons and Eqs. (3) and (4) were used to calculate the radial distribution of the energy density $Q(r)$:

$$\begin{aligned} Q(r) &= Q_0, \quad r < a, \\ &= Q_0 (a/r)^{\alpha}, \quad a < r < R_{\max}, \end{aligned} \tag{6}$$

where a is a quantity of the order of the interatomic distance and $\alpha \approx 2$. The factor Q_0 is found from the normalization condition

$$2\pi N \int_0^{\infty} Q(r)\, r\, dr = \left(\frac{dE}{dx}\right)_e. \tag{7}$$

The quantity $R_{\max}$ depends on the maximum energy $E_{\max}$ which an electron may acquire and it ranges from $R_{\max} = 1$ nm for heavy ions to $R_{\max} \approx 10$ nm for light ions. We can see from Fig. 2 that $R(E)$ varies slowly at low energies E and in the case of heavy ions the density Q is approximately proportional to $(dE/dx)_e$, whereas in the case of light ions the $Q(E)$ curve is shifted compared with $\left[\frac{dE}{dx}(E)\right]_e$ toward lower energies, since $R(E)$ increases on increase in E. Therefore, in the case of light ions the sputtering coefficient depends not only on $(dE/dx)_e$, but also on the primary electron spectrum, i.e., on the ion energy E. The case of high energy densities, when Q is greater than the characteristic energy for the excitation of electrons and a plasma of hot electrons forms in the hot region, has been investigated thoroughly.[10] The electron-electron collision time in the conduction band is $\sim 10^{-16}$ s, whereas the ionization time of atoms by electron impact is 10^{-15} s and an ionization equilibrium is established in this time. Vacancies in the inner shells, formed by fast ions, are filled as a result of the Auger processes in a time $\sim 10^{-14}$ s, but the concentration of such vacancies is relatively low and the total neutralization energy is much less than the excitation energy Q. An equilibrium energy distribution of electrons excited above the bottom of the conduction band is also established in $\sim 10^{-16}$ s. At high values of Q the properties of an excited electron gas differ considerably from the properties of an electron gas in a metal at room temperature. Approximate expressions for the average energy $\langle \varepsilon \rangle$ and the equation of state of an electron gas at an arbitrary temperature were obtained in Ref. 68:

$$\langle \varepsilon \rangle = \frac{TF_{3/2}(\eta)}{F_{1/2}(\eta)} \approx \frac{3}{2}(T^2 + 0.16\varepsilon_F^2)^{1/2}, \tag{8}$$

where

$$F_{k+(1/2)} = \int_0^{\infty} (e^{x-\eta} + 1)^{-1} x^{k+(1/2)}\, dx$$

is the Fermi integral; $\eta = \mu(T)/T$; $\mu(T)$ is the chemical potential; $\mu(0) = \varepsilon_F$; T is the electron temperature. The pressure in an electron gas is

$$P = \frac{2}{3} n \langle \varepsilon \rangle \approx n \left[T^2 + \frac{(3\pi^2)^{1/3} \hbar^4 n^{4/3}}{25 m^2} \right]^{1/2}, \tag{9}$$

where $n = Z(T)N$; $Z(T)$ is the average number of electrons per atom in the conduction band; N is the number of atoms per unit volume. The average charge $Z(T)$ can be determined from the Saha distribution. A simple approximation for $Z(T)$ was proposed in Ref. 10:

$$\begin{aligned} Z(T) &= Z_0 \frac{T}{T_*}, \quad T > T_*, \\ &= Z_0, \quad T < T_*, \end{aligned} \tag{10}$$

where Z_0 is the number of electrons in the conduction band at $T = 0$. The characteristic temperature T_* varies somewhat from substance to substance, but in the majority of cases it is within the range $5 \text{ eV} < T_* < 10 \text{ eV}$. In the case of insulators at temperatures $T < g$, we have $Z \approx \exp(-g/2T)$, where g is the width of the band gap.

The Debye screening radius d_0 of an excited region is given by an approximate expression, similar to Eqs. (8) and (9), which gives the correct asymptote and ensures that the error does not exceed 10%:

$$d_0^2 \approx \frac{[T^2 + (2/3)^2 \varepsilon_F^2]^{1/2}}{4\pi n e^2}. \tag{11}$$

In view of the dependence $n(T)$, the screening radius d_0 of metals increases somewhat with temperature in the range $T < \varepsilon_F$ and then remains constant amounting to $d_0 = 0.7$–0.8 Å. In the case of insulators, when $T < g$, we have $n = ZN \propto \exp(-g/2T)$ and the Debye radius first falls on increase in temperature and then remains constant and equal to the value for metals.

On increase in the temperature T there is an increase in the total potential excitation energy of electrons:

$$U(T) = \sum_Z C_Z(T) \sum_k^Z J_k, \tag{12}$$

where J_k is the potential for the excitation of the k shell electrons to the conduction band and $C_Z(T)$ is the concentration of ions with a charge Z.

The total energy of the electron subsystem is equal to the sum of the potential energy $U(T)$ and the kinetic energy of electrons excited above the bottom of the conduction band.

$$Q = Z(T) \langle \varepsilon(T) \rangle + U(T). \tag{13}$$

Knowing the dependence $U(T)$, we can use the solution of Eq. (13) to find the initial electron temperature T_0 and the initial average charge of ions $Z(T_0)$ for a given value of $Q - Q_0$. For example, in the case of a region excited by a fission fragment of ^{252}CF in gold, we have $Q_0 = 130$ eV, $T_0 \approx 20$ eV, and $Z(T_0) = 3$.

Therefore, in the case of metals and insulators when Q_0 exceeds the Fermi energy ε_F and the band gap g the initial

excitation region represents a plasma containing hot electrons and cold inmobile ions. However, relaxation of the excited region is due to different processes in metals and insulators.

The situation is different in the case of low values of Q_0. In the case of metals when $Q_0 < \varepsilon_F$, single-particle excitations are distributed between several low-energy electrons characterized by a large range (Fig. 2), so that energy is spread over a large volume. The whole relaxation process lasts $\sim 10^{-15}$ s. Plasma oscillations at distances ~ 10 nm also dissociate into single-particle excitations of electrons near the Fermi surface. Therefore, in fact an excitation region is not observed in metals at all when Q is low.

Collective excitations in molecular crystals dissociate and transfer their energy to one molecule. If the excitation energy is higher than the ionization potential, direct ionization takes place or superexcited states[69] are formed and these in turn dissociate along the following channels[29]:

$$\begin{aligned}
\mathrm{ABC} &\xrightarrow{\hbar\omega > J_1} \mathrm{ABC^+ + e^-} \text{ — direct ionization,}\\
&\rightarrow \mathrm{ABC^{**}} \text{ — formation of superexcited states,}\\
&\rightarrow \mathrm{AB^* + C} \text{ — predissociation,}\\
\mathrm{ABC^{**}} &\rightarrow \mathrm{ABC^+ + e^-} \text{ — atomization,}\\
&\rightarrow \mathrm{ABC} + \Delta E_{\mathrm{vibr}} + \hbar\nu \text{ — radiative relaxation,}\\
&\rightarrow \mathrm{ABC} + \Delta E_{\mathrm{vibr}} \text{ — nonradiative relaxation.}
\end{aligned}$$

Therefore, single dissociated molecules and molecules in excited vibrational states form in the excitation zone. Moreover, direct ionization by an ion and dissociation of collective excitations creates molecular ions.

Only isolated excitations of the exciton type appear in ionic crystals at low values of Q_0. In this case the process of inelastic sputtering is due to mechanisms similar to the mechanisms of the sputtering by electrons[1)] with subthreshold energies or by γ photons, discussed in a recent monograph.[8] Therefore, we shall ignore inelastic sputtering at low values of Q_0. We shall simply mention that light ions, like electrons of subthreshold energies, cause inelastic sputtering of just some insulators. The mechanisms of such sputtering are associated with the direct transfer of the energy of an excited electron to atoms or molecules.

At average energies of $Q \sim 1$–10 eV/atom the regions of isolated excitations alternate along ion tracks with plasma regions and this is due to fluctuations of the energy losses represented by $(dE/dx)_e$. In this case the process of sputtering is governed by the probability of formation of a region with a high value of Q near the surface.[70]

The problem of the charge distribution in an excited region is of major interest. It was first suggested in Ref. 71 and then in other papers that primary excited δ electrons leave the ionization region where positive ions remain. This hypothesis has been used to formulate the concept of a Coulomb explosion, i.e., flying apart of ions under the action of repulsion forces. However, it has been shown already[52,71,72] that the Coulomb explosion mechanism does not apply to metals because the sufficiently high conductivity ensures neutralization of a positively charged region in a time of the order of $\omega_p^{-1} = (4\pi ne^2/m)^{1/2} \approx 10^{-16}$ s, which is considerably less than the time necessary for the acquisition of the sputtering energy by an ion.

It is assumed in Refs. 71 and 73–75 that the formation of tracks in insulators irradiated with nuclear fission fragments or multiply charged ions is due to the Coulomb explosion mechanism. It is assumed in Refs. 73–75 that the neutralization of ions can only be due to free electrons, and since there are practically no free electrons in insulators, the neutralization does not take place. However, according to Ref. 72, electrons are returned by the Coulomb field to a positively charged region well before ions can acquire an energy sufficient for flying apart. The relaxation of electrons to the valence band or their capture by local levels are also much slower processes than the return to positive ions. This is true of a cylindrical excited region created by a fast ion, because the potential energy of an electron increases away from a positively charged cylinder. At low values of $(dE/dx)_e$, when the number of ionization events per unit track length $(dE/dx)_e/J$ is small and the distance between the ions which are formed $J/(dE/dx)_e$ is greater than the distance r of an electron from an ion, it follows that an electron in an insulator can be captured by a local level after it loses its energy. This creates an uncompensated positive ion. However, even in this case the distance between ions is large and the Coulomb repulsion is weak.

The presence of a positive charge is possible also in a hemispherical region created by a slow multiply charged ion when it becomes neutralized at the surface. The positive charge is contributed by a multiply charged ion itself and it is also formed as a result of electron emission.

The conductivity inside an excited region has the effect that the charge is distributed on its boundary. This creates an electric field $|\mathbf{E}| \approx Q/R^2$, which in the case of large charges Q in the excited region may accelerate ions in the surface layer and supply them with an energy sufficient for sputtering.

4.2. Relaxation of electron excitation and models of sputtering of metals

The main processes of relaxation of an electron excitation at high values of Q in metals are the electron heat conduction and the transfer of energy to atoms in the crystal lattice. The rates of these processes were first estimated back in 1959 (Ref. 77). It was shown in Ref. 77 that the cooling of electrons because of electron heat conduction is much faster than the transfer of energy to atoms and, for example, near a track of a fission fragment in a metal the temperature of the atoms rises by just 1–10 K. However, an electron thermal diffusivity $\chi \approx 100$ cm^2/s, typical of metals at room temperature, was used in Ref. 77. It was shown later[68] that the electron thermal diffusivity has a deep minimum at $T \approx 10$ eV (Fig. 19), where $\chi \sim 1$ cm^2/s is two orders of magnitude less than in metals under normal conditions. The dependence

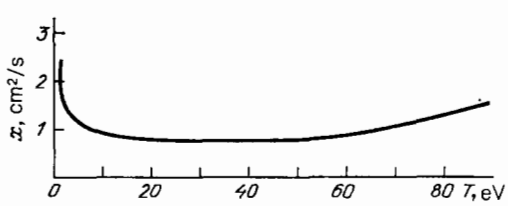

FIG. 19. Temperature dependence of the electron thermal diffusivity $\chi(T)$.[68]

$\chi(T)$ is governed mainly by the cross section for electron-electron collisions:

$$\chi_e \approx \frac{\lambda_{ee}\bar{v}}{3} \approx \frac{\bar{v}}{3n\sigma}. \quad (14)$$

If $T<\varepsilon_F$, it follows from the Pauli principle that $n \propto (T/\varepsilon_F)^2$; σ is the transport cross section for collisions between two electrons. At low energies we have $\sigma \approx$ const, whereas in the range $T \gg \varepsilon_F$ the cross section for pair electron-electron collisions and plasmon excitation decreases on increase in the electron energy. This is the reason for the minimum of $\chi(T)$.

It therefore follows that the characteristic cooling time of electrons in an excited region is $t_1 = R^2/4\chi \approx 10^{-15}$ s due to electron heat conduction. At high temperatures the number of electrons in the conduction band $n(T)$ falls as a result of cooling because of recombination of ions via the Auger processes and the potential energy is converted into the thermal energy of electrons which remain in the conduction band. The result is slower cooling of the excited region.

The time τ for the transfer of energy from hot electrons to the lattice was calculated on a number of occasions.[10,78,79] If τ_{coll} is the electron-phonon collision time, then

$$\tau^{-1} = \frac{\delta}{\tau_{coll}}, \quad (15)$$

where δ is the fraction of the electron energy transferred to the lattice in one collision. It was found in Ref. 78 that at a lattice temperature Θ higher than the Debye temperature Θ_D this fraction is $\delta = 2ms^2/\Theta$, where s is the velocity of sound. The authors of Ref. 10 considered the possibility of multiphonon excitation and found that $\delta = (2ms/3p)(\Theta_D/\Theta)$, where the electron momentum is $p > \Theta_D/s$. Since in a defect-free crystal an electron can be scattered only by phonons, i.e., by atoms shifted from the equilibrium position, it follows that

$$\tau_{coll,1}^{-1} = Nv\sigma\,\overline{(\Delta\mathbf{k}\cdot\Delta\mathbf{r})^2}, \quad (16)$$

where N is the number of atoms per unit volume; v is the velocity of an electron; σ is the cross section for the scattering of an electron by an isolated atom; $\Delta\mathbf{k}$ is the change in the wave vector of an electron as a result of the scattering; $\Delta\mathbf{r}$ is the displacement of an atom from its equilibrium position as a result of thermal vibrations. The time for the transfer of energy from electrons to the lattice is $\tau_1 \approx 10^{-12}$ s, which is long because of the smallness of the fraction δ of the energy transferred in one collision and because of the factor $\overline{(\Delta\mathbf{k}\cdot\Delta\mathbf{r})^2} \sim 10^{-2}$, which governs the number of collisions of electrons with phonons.

The characteristic cooling time of electrons in metals due to heat conduction is $t_1 \approx 10^{-15}$ s, which is considerably less than the time τ_1 for the transfer of the electron energy to the lattice. A rough estimate shows that the lattice temperature can rise to

$$\Theta \approx (t_1/\tau_1)\,T_0 \approx 10^{-3}\,T_0 \sim 100\ \text{K}.$$

It therefore follows that in an ideal metal crystal there should be no damage as a result of inelastic losses experienced by a fast ion, as confirmed by the absence of visible tracks of fission fragments. Inelastic sputtering of metals can be explained only if we postulate special mechanisms of the transfer of the electron energy to atoms. The existing models of inelastic sputtering can be divided into two groups: the thermal spike models[28,35,80,81] and the Coulomb explosion models.[71,73,75] Neither of these models can be applied to metals in the original form. Electrons cannot heat a crystal to temperatures needed in sputtering and since there is no space charge in an excited region, there is no Coulomb repulsion of ions. Nevertheless, the later thermal spike models deal with special cases when a more intensive transfer of energy from electrons to atoms is possible and the Coulomb explosion models are based on the idea of ion acceleration in an electric field.

The modernized thermal spike models are based on the assumption that a crystal is imperfect and that a reduction in the electron-lattice relaxation time is due to the scattering of electrons by defects.[82]

In the simplest variant the electron-lattice interaction coefficient is selected so that during the cooling time of an excited region the lattice acquires the necessary energy because of electron conduction.

The selection of this electron-lattice interaction coefficient is justified by a strong increase in the sputtering coefficient of fine-grained materials on reduction in the grain size.[35,41] The sputtering coefficient increases when the grain size becomes comparable with the mean free path of electrons λ_{eff} in the case of the electron-phonon interactions. It is therefore assumed in Refs. 42 and 83 that the time for the transfer of energy from electrons to the lattice in grains of size L decreases by a factor λ_{eff}/L. If we consider the case of a fine-grained (defect) structure of bulk materials,[82] we find that all the energy transferred by an incident atom to the electron subsystem of a single grain is "locked-in" in the grain if electrons are reflected from the grain boundary and the reflection coefficient is close to unity. However, the height of the potential barrier for electrons is governed by the difference between the work functions of different faces of adjacent grains and it amounts to several tenths of an electron volt, whereas in the case of boundaries covered by an oxide layer it amounts to ~ 1 eV. The width of such a barrier is of the order of the interatomic distance. Therefore, electrons may be reflected from a grain boundary only after cooling to a temperature of $T \sim 1$ eV. If the electron energy is greater than the height of the potential barrier, the electron reflection coefficient should be approximately the same as in the case of reflection of electrons undergoing emission from an internal surface in a crystal[84]; in this case the reflection coefficient does not exceed ~ 0.3, so that we cannot use the concept of locked-in electrons.

On the other hand, the model of an isolated grain can be used to explain experiments on fine-grained coatings,[13,15,42,83,85,86] when single grains of small size have small areas of contact with the metal substrate. Single grains cool slowly also on an insulating substrate.

If we assume that the energy released in a grain is locked completely inside the grain, we obtain an expression[35,42,83] for the sputtering coefficient of a fine-grained coating with a known grain size distribution:

$$S = \frac{4\pi^2 N}{3\Pi} \sum_i f_i R_i^5 \left\{1 - \left[\frac{(4/3)\,\pi R_i^3 N u_0}{2R_1\,(\mathrm{d}E/\mathrm{d}x)_e}\right]^2\right\}, \quad (17)$$

where f_i is the number of grains with a radius R_i on a substrate of area A. Equation (17) is derived assuming that the

whole grain evaporates and that sputtering occurs if each atom acquires an energy greater than the sublimation energy U_0. However, a comparison of the above expression with the experimental results has shown that U_0 should be replaced with a certain effective value U_{eff}, which is less than U_0. It means that in reality we can expect detachment of clusters of atoms or of whole grains. This may occur because of the repulsion between the hot periphery of a grain and the substrate.

The model of grain detachment was developed in detail in Refs. 10 and 87 and it was shown there that electrons heat the lattice much more strongly near a grain boundary than inside the grain. Excited thermalized electrons moving in a periodic potential are described by the Bloch wave functions and the electron-phonon collision time is given by Eq. (16). However, when an electron crosses a grain boundary and reaches a neighboring grain after traveling its mean free path λ, before it has lost its directional momentum we can regard it as a free particle. The time for the collision of an electron with the lattice atoms is

$$\tau_{\text{coll},2} = (N\sigma v)^{-1}, \tag{18}$$

i.e., $\overline{(\Delta \mathbf{k}\cdot\Delta \mathbf{r})}^2$ times less than the time $\tau_{\text{coll},1}$ for the collision of an electron with the lattice inside a grain; there is a corresponding reduction in the time for the transfer of the electron energy to the lattice, which near a grain boundary is

$$\tau_2 = \tau_{\text{coll},2}\delta^{-1}. \tag{19}$$

Consequently, the lattice atoms located at a distance λ from the grain boundary, near the point where it is crossed by, for example, a fission fragment, are heated to a temperature $\Theta \sim 1$–2 eV.

If the force of repulsion between grains,

$$F = 2\pi \int_0^\infty \frac{2}{3}\,\theta N r\,dr > \pi\gamma L^2, \tag{20}$$

exceeds the surface tension force, a grain becomes detached from the target. This condition makes it possible to find the maximum radius L_m of a spherical grain which may be detached from the target by a fast ion. In the case of sputtering of fine-grained gold by ^{252}Cf fragments, we have $L_m \approx 100$ Å, which corresponds to the maximum sputtering coefficient $S = (4\pi/3)L_m^3 N \approx 1.5\cdot 10^5$ atoms/fragment. This mechanism for the detachment of fine grains agrees with the observed strong dependence of the sputtering coefficient on the grain size. The model in question accounts for the formation of fission fragment tracks in fine-grain metals[88] and also for the sintering of grains as a result of irradiation with fission fragments.[89] The detachment of grains is attributed in Refs. 90 and 91 to their "shaking-off" by a shock wave created by an ion in a nonconducting substrate or to "jumps" due to fast thermal expansion.

The initial Coulomb explosion idea has been transformed to a model of acceleration of ions in an electric field which appears even when an excited region is on the whole quasineutral. The assertion that "a sufficiently strong electric coupling between ions and electrons represents a bulk force acting on matter" was first put forward in Ref. 92, so that we can assume that ions acquire the following velocity during the lifetime of an excitation:

$$U = \frac{1}{MN}\int_0^\infty \frac{\partial P(r,\,t)}{\partial r}\,dt, \tag{21}$$

where P is the electron pressure and M is the ion mass. Although the electric force was not made more specific in Ref. 92, Eq. (21) essentially means ($P = NZT$) that the plasma potential is $\varphi \approx T/e$ and a force $Ze\nabla\varphi$ acts on each ion. However, in view of the fairly high thermal diffusivity, the temperature gradient decreases rapidly and the velocity of Eq. (21) acquired by an ion is insufficient for its displacement.

The effects of the electron pressure on atoms were considered in Ref. 66 using a modified potential model. The mechanism of these effects was again unspecified and the pressure calculations were made using an expansion of the average energy in terms of the electron temperature T, which is justified only if $T/\varepsilon_F \ll 1$.

An excited region is regarded in Ref. 72 as a two-component plasma with cold ions and hot electrons. The authors of Ref. 72 calculated the response of an initially homogeneous system to the motion of an electron and estimated the energy losses suffered by the electron. Their calculations showed that because of the polarization of the plasma, the energy acquired by an ion of mass M and with a charge Z in a unit time is

$$\left.\frac{dE}{dt}\right|_{\text{ion}} = \frac{e^2\omega_p^2}{2v}\,\frac{mZ}{M}\left[\ln(1+x) - \frac{x}{(1+x)}\right], \tag{22}$$

where is the plasma-electron frequency; $\omega_p = (4\pi ne^2/m)^{1/2}$; $x = (vk_{\max}/\omega_p)^2$; $\hbar k_{\max} = 2mv$ is the maximum momentum transferred in a collision of an electron with an ion; v is the electron velocity. It follows from Eq. (22) that electrons of 10 eV energy in a plasma created by a 1-MeV He^+ ion in solid argon transfer ~ 1 eV to the ions in $\sim 10^{-12}$ s. However, it should be pointed out that this rate of lattice heating is comparable with the rate of heating by the electron-phonon interactions. Moreover, dealing with the heating of the lattice by electrons we have to allow also for other mechanisms of relaxation of the excited region.

The strongest electric field appears on the surface of an excited region in a metal.[10,87] In view of the high temperature and pressure of electrons a negative cloud of electron charges appears above the surface of a hot spot and the surface layer of ions is no longer compensated by electrons, i.e., a double electrical layer is formed and inside this layer the charges are separated by distances of the order of the Debye radius d_0. Since the Debye radius is much less than the distance at which the electron pressure falls at right-angles to the ion path [$d_0 \ll P(\partial P/\partial r)^{-1}$], the field on the surface is considerably stronger than the radial field E_r. The electric field pressure $E^2/8\pi$ inside such a double layer is balanced out by the electron gas pressure nT. More accurate estimates of the electric field on the surface give

$$E(0) \approx 3\,(P(-\infty))^{1/2}, \tag{23}$$

where $P(-\infty) = Tn(-\infty)$ is the electron gas pressure inside the metal at temperatures $T > \varepsilon_F$. Therefore, the ions in the surface layer experience a force

$$F = 3eZ(T)\,(nT)^{1/2}, \tag{24}$$

where $Z(T)$ is the average charge of an ion.

Under normal conditions the surface ions are held to-

gether by binding forces. The binding energy of a surface atom U_0 is defined as the difference between the energy per one atom in the lattice of a solid and the ionization energy of an isolated atom (see, for example, Ref. 93).

An increase in the electron temperature increases the average energy of electrons and the energy per one atom in a crystal (all the other terms in the energy of an atom in the lattice are independent of the electron temperature), so that there is a reduction in the binding energy of an atom and at an electron temperature[94]

$$T > T_c = \left(\frac{4}{9}U_0^2 + \frac{8}{15}U_0\varepsilon_F\right)^{1/2} \tag{25}$$

the binding energy $U(T)$ vanishes (U_0 is the binding energy of an atom at $T=0$). Typical values of this critical temperature T_c are 3–5 eV.

If the initial temperature T_0 in a hot spot is considerably higher than T_c, then after a time t_c, when the electron temperature falls to T_c, an ion experiences only the force of Eq. (24), which causes its detachment from the surface. Therefore, an ion acquires an energy

$$W(r,\ t) = W_0 F\left(\frac{r}{R_0}\right), \tag{26}$$

$$W_0 = \frac{0{,}14e^2}{\chi^2 M T_* n_0}\left(\frac{dE}{dx}\right)_e^2 \ln\frac{T}{T_c}. \tag{27}$$

The function $F(r/R_0)$ found in the range $0 < r/R_0 < 2$ is readily approximated by the following expression:

$$F = \left[1 + \frac{3}{2}\left(\frac{r}{R_0}\right)^2\right]^{-1}. \tag{28}$$

If the energy of a surface atom is greater than the binding energy $W > U_0$, the atom is released from the surface and the sputtering coefficient is then[94]

$$S = \frac{3}{2}\pi R_0^2 N^{2/3}\left(\frac{W_0}{U_0} - 1\right). \tag{29}$$

Therefore, the sputtering of metals has a threshold. The process can begin if the inelastic energy losses $(dE/dx)_e$ exceed a certain threshold value corresponding to $W_0 = U_0$. However, if $W_0 \gg U_0$, we find that $S \propto (dE/dx)_e^2$. An average fission fragment is characterized by $(dE/dx)_e \approx 25$ keV/nm in gold and we then have $S \approx 20$ atoms/fragment so that the threshold value is $(dE/dx)_e = 21$ keV/nm. This value of S is close to that found experimentally,[40,43] but because of indeterminacy of the parameters occurring in the expression for this quantity and because of the experimental errors, it is not yet possible to determine reliably whether inelastic sputtering of coarse-grained metals takes place. The most decisive experiments would be those yielding the energy dependence of the sputtering coefficient $S(E)$.

We may mention also that the angular distribution of sputtered atoms deduced on the basis of this model should be highly directional and concentrated near the normal to the surface; the angular width of the distribution should be

$$\Delta\varphi \approx \left(\frac{\Theta_0}{W_0 - U_0}\right)^{1/2}, \tag{30}$$

where Θ_0 is the target temperature.

We can see that the inelastic sputtering of metals has been described by a number of models and this clearly corresponds to the multipiicity of the mechanisms of erosion as a result of inelastic processes. Obviously, the exceptionally high sputtering coefficients of fine-grained metals are due to some special sputtering mechanisms. Erosion is likely as a result of detachment of whole grains.[35,37,55] However, on the surface of a grain which is in loose contact with the substrate the acceleration of ions in the field of a double layer is even more effective because of the slow cooling as a result of loss of heat across the contact with the substrate.[87] This should result in sputtering in the form of atoms, as postulated initially in the isolated grain model.[35,83] In the case of inelastic sputtering of coarse-grained metals the most plausible is the mechanism of acceleration of ions in the field of a double layer.

4.3. Relaxation of the excited region and sputtering of insulators

A fast multiply charged ion characterized by a high value of $(dE/dx)_e$ forms an excited region in an insulator and the parameters of this region are not very different from those of an excited region in a metal. The average ion charge Z and the initial electron temperature T_0 in the conduction band reach the same values at high energy densities Q_0 as in metals. Therefore, the thermal diffusivity of electrons χ in an excited region in the case when $Z \geqslant 1$ has the value $\chi \approx 1$ cm^2/s, exactly as in the case of metals at temperatures $T \gtrsim \varepsilon_F$.

However, the mechanism of heat transfer is different for metals and insulators. In metals the heat conduction due to electrons essentially results in the replacement of hot electrons on the axis of an excited region with cold electrons from the periphery of the region. In semiconductors with a high hole mobility the process of relaxation may be ambipolar diffusion with a diffusion coefficient close to χ for metals.

The situation is different in an insulator where positive charges are immobile and there are no free electrons outside the excited region. In view of the condition of quasineutrality, electrons cannot leave the excited region because they are held back by the Coulomb attraction.

The correct mechanism of the relaxation of the energy of excited electrons in an insulator was first identified in Ref. 66. Electrons can transfer their energy to bound electrons, i.e., they can ionize atoms at the periphery of an excited region and this results in expansion and relaxation of this region. The process ceases when the electron temperature becomes less than the band gap g. Cooling is described in Ref. 66 by the heat conduction equation with an effective coefficient

$$\chi = \frac{a^2}{3\tau_i} \tag{31}$$

where $\tau_i = (\pi\hbar^3/2e^4m)(N/n)(g/T)^2\exp(g/T)$ is the time for the excitation of an electron to the conduction band and a is the atomic size.

The process of relaxation in a region containing excited electrons in an insulator was investigated in Ref. 86 and it was found that expansion of such an excited region occurs because of an ionization wave. If the electron temperature T is greater than the band gap g, the wave velocity U and the width of a front l are[95]

$$U = 2\left(\frac{D}{\tau_i}\right)^{1/2}, \quad l = 2(D\tau_i)^{1/2}, \tag{32}$$

where D is the diffusion coefficient of electrons. The velocity U in an insulator is usually of the order of the thermal velocity of the electrons and if $T > g$, an ionization wave travels quite rapidly. However, as soon as the electron temperature falls to the value $T < g$, then because of a change in the electron distribution function[86] at the boundary of an excited region an ionization wave becomes modified. The front of the wave becomes steeper, the plasma becomes polarized, and free electrons escape from the excited region to a distance of the order of the Debye radius d_0 and they form a double layer. Since d_0 is less than the mean free path of electrons, the width (thickness) of the ionization front becomes $\sim d_0$ and the wave velocity is then

$$U \approx \frac{d}{\tau_1}. \tag{33}$$

When temperature is reduced, we find that $n \propto \exp(-g/2T)$, and the average ionization time increases $\tau_i \propto \exp(3g/2T)$, so that

$$U \propto \exp\left(-\frac{5g}{4T}\right), \tag{34}$$

i.e., at low temperatures an excitation region relaxes slowly.

If $T > g$, when practically all the atoms are ionized in an insulator, the transfer of the electron energy to the lattice in metals and insulators proceeds in the same manner. However, if $T < g$, when the number of ions in an excited region is small, we have $n/N < 1$, and the scattering of an electron by an ion occurs as in a gas, because the potential of an ion differs from the potential of a neutral atom. The electron-lattice collision time is then

$$\tau_{\text{coll}} = (nv\sigma)^{-1} \tag{35}$$

and it differs from Eq. (16) because the periodicity of the potential is disturbed by the random distribution of ions.

We can assume that the excitation energy is transferred to atoms in a crystal inside a volume of radius $R(T_1)$ if the cooling time of this volume $R(T_1)/U(T_1)$ is equal to the time for the transfer of energy from electrons to the lattice $\tau(T_1)$ given by

$$\tau(T_1) = \frac{R(T_1)}{U(T_1)}. \tag{36}$$

A root of Eq. (36) gives the temperature to which the atoms in a crystal are raised:

$$\Theta \approx \frac{n(T_1)}{N}\left(T_1 + \frac{2g}{3}\right). \tag{37}$$

In most cases the value of Θ is less than the binding energy of surface atoms and these atoms cannot escape. However, Θ usually exceeds the melting point so that fission fragment tracks are observed in insulators.

The specific sputtering mechanism of insulators is not yet clear. The spectrum of the energies of sputtered particles can most probably be explained by the evaporation of surface atoms. Rapid heating of a bounded region can give rise to the formation of a shock wave, which on escape to the surface transfers an energy sufficient for the sputtering of atoms or a group of atoms.[90,96,97] This mechanism explains well the narrow angular distribution of the sputtered particles.

The sputtering of fine-grained insulators characterized by large sputtering coefficients is clearly due to special mechanisms. These mechanisms may include detachment of a grain, similar to that investigated in the case of metals, and the size of the grains detached from metals and insulators should be of the same order of magnitude. However, excited electrons in an insulator grain which is in poor contact with the substrate relax more slowly than in a metal and this may result in stronger sputtering of isolated grains in the form of atoms.

In the case of slow multiply charged ions when the neutralization energy is released near the surface an excited region may also relax in the form of an ionization wave. This problem has not yet been investigated in detail, because we cannot exclude the formation of a space charge or the Coulomb repulsion of ions. If the energy of an ion in an insulator exceeds the displacement energy E_d, the subsequent evolution of the process can be regarded as a cascade of collisions[74,98] or direct emission of accelerated ions. In the opposite case, we can expect evaporation of matter from the surface of the heated region.[60] However, this topic requires further study.

The transfer of energy from electrons to atoms and molecules in molecular crystals may be due to the excitation of vibrational levels of the molecules and dissociative recombination. In a study of the relaxation process in a track of a heavy ion in a molecular crystal[99] an analysis was made of a system of kinetic equations for electrons, ions, and neutral molecules allowing both for attraction and reactions. For a certain selection of cross sections, coupling constants, and reactions the total energy of such a system is negative, which shows that bound states can form (these can be clusters or ordered distributions of particles, such as those in a quasimetal structure). Lowering of the degree of ionization increases the energy of the system, which becomes positive and this can be interpreted[99] as decay of bound states accompanied by heating of the atomic subsystem. The process of dissociative recombination is suggested as the mechanism of the transfer of energy of electrons to the atoms.[100-102] These processes are clearly the most probable for molecular crystals and liquids of the O_2, CO_2, N_2, and H_2O types. Then, because of the large cross sections of dissociative recombination the process of transfer of energy to atoms occurs in a time of $\sim 10^{-13}$ s (Ref. 102), which is less than the electron-phonon relaxation time. It follows that the sputtering of molecular crystals occurs when binding is lost due to dissociation of molecules and when the atomic subsystem is heated. However, this topic also needs a more thorough investigation.

It follows from the above discussion that the theory of inelastic sputtering of insulators is far from complete. Some specific topics have been dealt with and some general ideas on specific mechanisms of inelastic sputtering of nonconducting materials have been discussed.

5. CONCLUSIONS

It is obvious that we are at an early stage of studies of a new field and the outlines of this field as well as potential applications are only slowly becoming clear. Inelastic sputtering has already been observed for different objects on irradiation with different ions. It differs radically from elastic sputtering. The observed relationships governing inelastic sputtering are evidence that the effect has many facets. Excitation of the electron subsystem plays also an important role

in the desorption of impurities from the surface as a result of inelastic interaction with ions[89] and in the formation of radiation damage (tracks of particles, sintering of grain boundaries and layers), and it stimulates chemical reactions.

All these effects require, like inelastic sputtering, extensive experimental and theoretical investigations. Such investigations are particularly desirable because many applications of the new field are already clear.

Sputtering of high-molecular compounds in the form of large molecules or their fragments as a result of irradiation with fast ions or fission fragments provides a convenient method for mass spectrometric investigations of such compounds. The method is unique particularly in the case of biological objects.

The large difference (by two orders of magnitude) between the sputtering coefficients of insulators and conducting materials can be used for selective sputtering of insulators without erosion of semiconductors and metals when microelectronic components are being manufactured.

The sputtering by slow multiply charged ions is an important topic in the development of a thermonuclear reactor because heavy impurities in a thermonuclear plasma may acquire charges in the range $q > 20$.

Studies of inelastic sputtering help to understand the characteristic features of the excitation of the electron subsystem, which is important in studies of the interaction of laser and electron beams with solids.

Inelastic sputtering of solidified gases is of interest in astrophysics, because irradiation of space objects containing ice and solidified gases by high-energy particles results in sputtering characterized by very large coefficients ($S = 10^2$–10^3 atoms/ion).

The reliability of semiconductor devices, particularly those of the submicron size, is important when such devices are used in space and are thus exposed to cosmic rays with a heavy component that can cause inelastic sputtering.

It follows that although radiation physics has been concentrated mainly on elastic atomic collisions, the stress should now be on studies of inelastic processes.

[1)]The threshold energy of an electron is the energy $(4m/M)E$ needed to transfer to a target atom of mass M an energy E_d sufficient to displace this atom from the lattice site to an interstitial position.

[1]R. Behrisch (ed.), *Sputtering by Particle Bombardment*, I, Springer Verlag, Berlin, 1981 [Topics in Applied Physics, Vol. 47] [Russ. transl., Mir, M., 1984].
[2]B. M. Aleksandrov, I. A. Baranov, A. S. Krivokhatskiĭ, and G. A. Tutin, At. Energ. **33**, 821 (1972) [Sov. At. Energ. **33**, 941 (1972)].
[3]B. M. Aleksandrov, N. V. Babadzhanyants, I. A. Baranov, A. S. Krivokhatskiĭ, L. M. Krizhanskiĭ, and V. V. Obnorskiĭ, Preprint No. RI-24 [in Russian], Khlopin Radium Institute, Academy of Sciences of the USSR, Leningrad (1974).
[4]F. S. Lapteva and B. V. Ershler, At. Energ. **1**, No. 4, 63 (1956) [Sov. J. At. Energ. **1**, 513 (1956)].
[5]T. U. Arifov, E. K. Vasil'eva, D. D. Grinch, S. F. Kovalenko, and S. M. Morozov, Izv. Akad. Nauk SSSR Ser. Fiz. **40**, 2621 (1976) [Bull Acad. Sci. USSR Ser. Fiz. **40**, No. 12, 150 (1976)].
[6]T. U. Arifov, D. D. Grinch, and S. M. Morozov, Proc. Fifth All-Union Conf. on Interaction of Atomic Particles with Solids [in Russian], Part 1, Radio Engineering Institute, Minsk (1978), p. 200.
[7]V. L. Auslender, I. A. Baranov, B. N. Belyaev, *et al.*, Preprint No. RI-56 [in Russian], Khlopin Radium Institute, Academy of Sciences of the USSR, Leningrad (1976).
[8]R. Behrisch (ed.), *Sputtering by Particle Bombardment*, II, Springer Verlag, Berlin, 1983 [Topics in Applied Physics, Vol. 52] [Russ. transl., Mir, M., 198, 1986].
[9]B. A. Trubnikov and Yu. N. Yavlinskiĭ, Zh. Eksp. Teor. Fiz. **48**, 253 (1965) [Sov. Phys. JETP **21**, 167 (1965)].
Yu. V. Martynenko and Yu. N. Yavlinskiĭ, At. Energ. **62**, 80 (1987) [Sov. At. Energ. **62**, 93 (1987)].
[11]A. A. Dorozhkin and N. N. Petrov, Ion Auger Spectroscopy [in Russian], Kalinin Polytechnic Institute, Leningrad (1983).
[12]I. G. Kaplan and A. M. Miterev, Dokl. Akad. Nauk SSSR **280**, 127 (1985) [Dokl. Phys. Chem. (1985)].
[13]I. A. Baranov and V. V. Obnorskiĭ, Vopr. At. Nauki Tekh. Ser. Fiz. Radiats. Povrezhdeniĭ Radiats. Materialoved. No. 5(28), 50 (1983) [in Russian].
[14]I. A. Baranov and V. V. Obnorskiĭ, Problems in Materials Science of the Thermal Power Equipment of Atomic Power Stations [in Russian], Kalinin Polytechnic Institute, Leningrad (1984), p. 33.
[15]S. O. Tsepelevich and I. A. Baranov, Abstracts of Papers presented at Thirty-Seventh Conf. on Nuclear Spectroscopy and Structure, Leningrad, 1987 [in Russian], Nauka, L., 1987, p. 594.
[16]J. E. Griffith, R. A. Weller, L. E. Seiberling, and T. A. Tombrello, Radiat. Eff. **51**, 223 (1980).
[17]L. E. Seiberling, C. K. Meins, B. H. Cooper, J. E. Griffith, M. H. Mendenhall, and T. A. Tombrello, Nucl. Instrum. Methods Phys. Res. **198**, 17 (1982).
[18]P. Hakansson and B. Sundqvist, Radiat. Eff. **61**, 179 (1982).
[19]P. Hakansson, I. Kamensky, and B. Sundqvist, Nucl. Instrum. Methods Phys. Res. **198**, 43 (1982).
[20]W. Knippelberg, O. Becker, and K. Wien, Nucl. Instrum. Methods Phys. Res. **198**, 59 (1982).
[21]A. Albers, K. Wien, P. Duck, W. Treu, and H. Voit, Nucl. Instrum. Methods Phys. Res. **198**, 69 (1982).
[22]O. Becker, S. Della-Negra, Y. Le Beyec, and K. Wien, Nucl. Instrum. Methods Phys. Res. Sect. B **16**, 321 (1986).
[23]B. B. Cooper and T. A. Tombrello, Radiat. Eff. **80**, 203 (1984).
[24]J. Bottiger, J. A. Davies, J. L'Ecuyer, N. Matsunami, and R. Ollerhead, Radiat. Eff. **49**, 119 (1980).
[25]R. W. Ollerhead, J. Bottiger, J. A. Davies, J. L'Ecuyer, and H. K. Haugen, Radiat. Eff. **49**, 203 (1980).
[26]W. L. Brown, W. M. Augustyniak, E. Simmons, K. J. Marcantonio, L. J. Lanzerotti, R. E. Johnson, J. W. Boring, C. T. Reimann, G. Foti, and V. Pirronello, Nucl. Instrum. Methods Phys. Res. **198**, 1 (1982).
[27]W. L. Brown, L. J. Lanzerotti, K. J. Marcantonio, R. E. Johnson, and C. T. Reimann, Nucl. Instrum. Methods Phys. Res. Sect. B **14**, 392 (1986).
[28]F. Besenbacher, J. Bottiger, O. Graversen, J. Hansen, and H. Sorensen, Nucl. Instrum. Methods Phys. Res. **191**, 221 (1981).
[29]I. G. Kaplan and A. M. Miterev, Khim. Vys. Energ. **19**, 208 (1985) [High Energy Chem. (USSR) **19**, 165 (1985)].
[30]P. Duck, H. Fröhlich, N. Bischof, and H. Voit, Nucl. Instrum. Methods Phys. Res. **198**, 39 (1982).
[31]B. Nees, E. Nieschler, N. Bischof, P. Duck, H. Fröhlich, W. Tiereth, and H. Voit, Radiat. Eff. 77, 89 (1983).
[32]E. Nieschler, B. Nees, N. Bischof, H. Fröhlich, W. Tiereth, and H. Voit, Radiat. Eff. **83**, 121 (1984).
[33]P. Hakansson, I. Kamensky, and B. Sundqvist, Surf. Sci. **116**, 302 (1982).
[34]C. K. Meins, J. E. Griffith, Y. Qiu, M. H. Mendenhall, L. E. Seiberling, and T. A. Tombrello, Radiat. Eff. **71**, 13 (1983).
[35]I. A. Baranov, A. S. Krivokhatskiĭ, and V. V. Obnorskiĭ, Zh. Tekh. Fiz. **51**, 2457 (1981) [Sov. Phys. Tech. Phys. **26**, 1455 (1981)].
[36]I. A. Baranov and V. V. Obnorskiĭ, Vopr. At. Nauki Tekh. Ser. Fiz. Radiats. Povrezhdenii Radiats. Materialoved. No. 5(19), 35 (1981).
[37]M. D. Rogers, J. Nucl. Mater. **15**, 65 (1965); **16**, 298 (1965).
[38]G. Nilsson, J. Nucl. Mater. **20**, 215 (1966).
[39]M. D. Rogers, J. Nucl. Mater. **22**, 103 (1967).
[40]B. M. Aleksandrov, I. A. Baranov, N. V. Babadzhanyants, A. S. Krivokhatskiĭ, and V. V. Obnorskiĭ, At. Energ. **41**, 417 (1976) [Sov. At. Energ. **41**, 1072 (1976)].
[41]I. A. Baranov and V. V. Obnorskiĭ, At. Energ. **54**, 184 (1983) [Sov. At. Energ. **54**, 192 (1983)].
[42]I. A. Baranov and V. V. Obnorskiĭ, Radiat. Eff. **79**, 1 (1983).
[43]S. O. Tsepelevich, I. A. Baranov, V. V. Obnorskiĭ, and B. M. Aleksandrov, Abstracts of Papers presented at Thirty-Sixth Conf. on Nuclear Spectroscopy and Structure, Leningrad, 1986 [in Russian], Nauka, Leningrad, 1986, p. 402.
[44]B. M. Aleksandrov, N. V. Babadzhanyants, I. A. Baranov, A. S. Krivokhatskiĭ, L. M. Krizhanskiĭ, and G. A. Tutin, At. Energ. **36**, 139 (1974) [Sov. At. Energ. **36**, 171 (1974)].
[45]B. M. Aleksandrov, N. V. Babadzhanyants, I. A. Baranov, A. S. Krivokhatskiĭ, V. V. Obnorskiĭ, and G. A. Firsanov, Preprint No. RI-25 [in Russian], Khlopin Radium Institute, Academy of Sciences of the USSR, Leningrad (1974).
[46]B. M. Aleksandrov, I. A. Baranov, N. V. Babadzhanyants, A. S. Kri-

vokhatskiĭ, V. V. Obnorskiĭ, and G. A. Firsanov, Preprint No. RI-33 [in Russian], Khlopin Radium Institute, Academy of Sciences of the USSR, Leningrad (1975).
[47]B. M. Aleksandrov, I. A. Baranov, A. S. Krivokhatskiĭ, and G. A. Tutin, Prikl. Yad. Fiz. No. 4, 36 (1974).
[48]V. A. Bessonov, G. P. Ivanov, N. A. Grinevich, and E. A. Borisov, At. Energ. **40**, 395 (1976) [Sov. At. Energ. **40**, 477 (1976)].
[49]G. P. Ivanov, V. A. Bessonov, N. A. Grinevich, V. A. Popovichev, and E. A. Borisov, At. Energ. **47**, 15 (1979) [Sov. At. Energ. **47**, 516 (1979)].
[50]J. P. Biersack and E. Santner, Nucl. Instrum. Methods Phys. Res. **198**, 29 (1982).
[51]D. Fink, J. P. Biersack, M. Stadele, K. Tjan, R. A. Haring, and A. E. de Vries, Nucl. Instrum. Methods Phys. Res. Sect. B **229**, 275 (1984).
[52]W. L. Brown, L. J. Lanzerotti, J. M. Poate, and W. M. Augustyniak, Phys. Rev. Lett. **40**, 1027 (1978).
[53]J. P. Biersack and E. Santner, Nucl. Instrum. Methods **132**, 229 (1976).
[54]R. Kelly, Nov. Fiz. Tverd. Tela No. 10, 194 (1980).
[55]I. V. Vorob'eva, Ya. E. Geguzin, and V. E. Monastyrenko, Poverkhnost, No. 4, 141 (1986) [Phys. Chem. Mech. Surf. (1986)].
[56]D. F. Torgerson, R. P. Skowronski, and R. D. Macfarlane, Biochem. Biophys. Res. Commun. **60**, 616 (1974).
[57]R. D. Macfarlane and D. F. Torgerson, Science **191**, 920 (1976).
[58]B. Sundqvist, Nucl. Instrum. Methods Phys. Res. **218**, 267 (1983).
[59]P. Hakansson, I. Kamensky, M. Salehpour, B. Sundqvist, and S. Widdiyasekera, Radiat. Eff. **80**, 141 (1984).
[60]L. E. Seiberling, J. E. Griffith, and T. A. Tombrello, Radiat. Eff. **52**, 201 (1980).
[61]O. Becker and K. Wien, Nucl. Instrum. Methods Phys. Res. Sect. B **16**, 456 (1956).
[62]N. Furstenau, W. Knippelberg, F. R. Krueger, G. Weiss, and K. Wien, Z. Naturforsch. Teil A **32**, 711 (1977).
[63]I. A. Baranov and S. O. Tsepelevich, At. Energ. **61**, 265 (1986) [Sov. At. Energ. **61**, 809 (1986)].
[64]I. A. Baranov, S. O. Tsepelevich, and V. V. Obnorskiĭ, At. Energ. **60**, 62 (1986) [Sov. At. Energ. **60**, 85 (1986)].
[65]S. A. Nepiĭko, Physical Properties of Small Metal Particles [in Russian], Naukova Dumka, Kiev (1985), p. 146.
[66]C. C. Watson and T. A. Tombrello, Radiat. Eff. **89**, 263 (1985).
[67]A. M. Miterev, I. G. Kaplan, and E. A. Borisov, Khim. Vys. Energ. **8**, 537 (1974) [High Energy Chem. (USSR) **8**, 461 (1974)].
[68]Yu V. Martynenko and Yu. N. Yavlinskiĭ, Dokl. Akad. Nauk SSSR **270**, 88 (1983) [Sov. Phys. Dokl. **28**, 391 (1983)].
[69]R. L. Platzman, Radiat. Res. **17**, 419 (1962).
[70]T. A. Tombrello, Nucl. Instrum. Methods Phys. Res. Sect. B **229**, 23 (1984).
[71]R. L. Fleischer, P. B. Price, and R. M. Walker, J. Appl. Phys. **36**, 3645 (1965).
[72]R. Ritchie and C. Claussen, Nucl. Instrum. Methods Phys. Res. **198**, 133 (1982).
[73]E. S. Parilis, *Proc. Intern. Conf. on Atomic Collision Phenomena in Solids*, Brighton, England, 1969, publ. by North-Holland, Amsterdam (1970), p. 324.
[74]I. S. Bitenskiĭ, M. N. Murakhmetov, and É. S. Parilis, Zh. Tekh. Fiz. **49**, 1044 (1979) [Sov. Phys. Tech. Phys. **24**, 618 (1979)].
[75]P. K. Haff, Appl. Phys. Lett. **29**, 473 (1976).
[76]V. M. Agranovich, D. K. Daukeev, S. Ya. Lebedev, and É. Ya. Mikhlin, Zh. Eksp. Teor. Fiz. **61**, 1511 (1971) [Sov. Phys. JETP **34**, 805 (1972)].
[77]I. M. Lifshitz, M. I. Kaganov, and L. V. Tanatarov, At. Energ. **6**, 391 (1959).
[78]V. L. Ginzburg and V. P. Shabanskiĭ, Dokl. Akad. Nauk SSSR **100**, 445 (1955).
[79]M. I. Kaganov, I. M. Lifshitz, and L. V. Tanatarov, Zh. Eksp. Teor. Fiz. **31**, 232 (1956) [Sov. Phys. JETP **4**, 173 (1957)].
[80]L. T. Chadderton, D. V. Morgan, I. McC. Torrens, and D. van Vliet, Philos. Mag. **13**, 185 (1966).
[81]A. A. Davydov and A. I. Kalinichenko, Vopr. At. Nauki Tekh. Ser. Fiz. Radiats. Povrezhdeniĭ Radiats. Materialoved. No. 3(36), 27 (1985).
[82]Ya. E. Geguzin, M. I. Kaganov, and I. M. Lifshits, Fiz. Tverd. Tela (Leningrad) **15**, 2425 (1973) [Sov. Phys. Solid State **15**, 1612 (1974)].
[83]I. A. Baranov and V. V. Obnorskiĭ, Preprint No. RI-120 [in Russian], Khlopin Radium Institute, Academy of Sciences of the USSR, Leningrad (1980).
[84]L. N. Dobretsov and M. V. Gomoyumova, Emission Electronics [in Russian], Nauka, M., 1966.
[85]I. S. Bitenskiĭ, At. Energ. **49**, 232 (1980) [Sov. At. Energ. **49**, 682 (1980)].
[86]V. V. Katin, Yu. V. Martynenko, and Yu. N. Yavlinskiĭ, Pis'ma Zh. Tekh. Fiz. **13**, 665 (1987) [Sov. Tech. Phys. Lett. **13**, 276 (1987)].
[87]Yu. V. Martynenko and Yu. N. Yavlinskiĭ, Preprint No. 4084/11 [in Russian], Institute of Atomic Energy, M., 1985.
[88]R. L. Fleisher, P. Price and R. Walker, *Nuclear Tracks in Solids*, University of California Press, Los Angeles (1975).
[89]K. O. Legg, R. Whaley, and E. W. Thomas, Surf. Sci. **109**, 11 (1981).
[90]I. V. Vorob'eva, Ya. E. Geguzin, and V. E. Monastyrenko, Fiz. Tverd. Tela (Leningrad) **28**, 163 (1986) [Sov. Phys. Solid State **28**, 88 (1986)].
[91]I. V. Vorob'eva, Ya. E. Geguzin, and V. E. Monastyrenko, Izv. Akad, Nauk SSSR Ser. Fiz. **50**, 1597 (1986) [Bull. Acad. Sci. USSR Ser. Fiz. **50**, No. 8, 134 (1986)].
[92]I. P. Borin, Fiz. Tverd. Tela (Leningrad) **20**, 2222 (1978) [Sov. Phys. Solid State **20**, 1284 (1978)].
[93]G. Leibfried, "Gittertheorie der mechanischen und thermischen Eigenschaften der Kristalle," in: Handbuch der Physik (ed. by S. Flügge), Vol. 7, Part 1, Springer Verlag, Berlin (1955), pp. 104–324 [Russ. transl. Fizmatgiz, M., 1963].
[94]Yu. V. Martynenko and Yu. N. Yavlinskiĭ, Zh. Tekh. Fiz. **58**, 1164 (1988) [Sov. Phys. Tech. Phys. **33**, 683 (1988)]; Dokl. Akad. Nauk SSSR **270**, 88 (1983) [Sov. Phys. Dokl. **28**, 391 (1983)].
[95]A. A. Ivanov, V. V. Parail, and T. K. Soboleva, Zh. Eksp. Teor. Fiz. **64**, 1245 (1973) [Sov. Phys. JETP **37**, (1973)].
[96]Y. Hayashiuchi, Y. Kitazoe, T. Sekiya, and Y. Yamamura, J. Nucl. Mater. **71**, 181 (1977).
[97]I. S. Bitensky and E. S. Parilis, Nucl. Instrum. Methods Phys. Res. Sect. B **21**, 26 (1987).
[98]I. S. Bitenskiĭ and É. S. Parilis, At. Energ. **46**, 269 (1979) [Sov. At. Energ. **46**, 316 (1979)].
[99]A. M. Miterev, Khim. Vys. Energ. **14**, 483 (1980) [High Energy Chem. (USSR) **14**, 369 (1980)].
[100]R. E. Johnson and W. L. Brown, Nucl. Instrum. Methods Phys. Res. **198**, 103 (1982).
[101]D. I. Slovetskiĭ, Theoretical and Applied Plasma Chemistry [in Russian], Nauka, M., 1975, p. 113.
[102]I. G. Kaplan, A. M. Miterev, and L. M. Khadzhibekova, Khim. Vys. Energ. **11**, 409 (1977) [High Energy Chem. (USSR) **11**, 432 (1977)].
[103]L. C. Northcliffe and R. F. Schilling, Nucl. Data A **7**, 233 (1970).
[104]J. F. Ziegler (ed.), *The Stopping and Ranges of Ions in Matter*, Vol. 5, Handbook of Stopping Cross-Sections for Energetic Ions in All Elements, Pergamon Press, London (1980).
[105]J. A. La Verne and R. H. Schuler, J. Phys. Chem. **88**, 1200 (1984).
[106]J. Ziegler, Nucl. Instrum. Methods **168**, 17 (1980).
[107]I. A. Baranov and S. O. Tsepelevich, Vopr. At. Nauki Tekh. Ser. Fiz. Radiats. Povrezhdeniĭ Radiats. Materialoved. No. 1(39), 75 (1987).

Translated by A. Tybulewicz